Science of the Total Environment 650 (2019) 2778–2795

Contents lists available at ScienceDirect

Science of the Total Environment

journal homepage: www.elsevier.com/locate/scitotenv

# Projection of temperatures and heat and cold waves for Aragón (Spain) using a two-step statistical downscaling of CMIP5 model outputs

Emma Gaitán [a,b], Robert Monjo [b], Javier Pórtoles [b], Mª. Rosa Pino-Otín [a,*]

[a] Universidad San Jorge, Villanueva de Gállego, 50830, Zaragoza, Spain
[b] Fundación para la Investigación del Clima, C/Tremps 11, 28040 Madrid, Spain

## HIGHLIGHTS

- Future temperature and heat and cold wave scenarios are obtained for Aragón, Spain.
- All scenarios are obtained using Earth System Models from CMIP5 for the first time.
- Intensity and duration of the cold waves will remain stable during this century.
- Intensity and duration of the heat waves will increase (3.6 °C, 7 days).
- The maximum temperature may increase up to 7 °C in summer at the end of the century.

## GRAPHICAL ABSTRACT

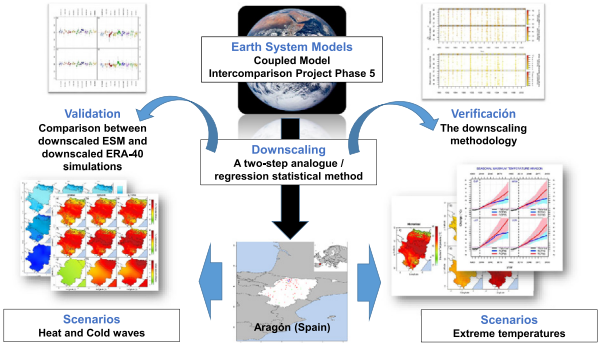


## ARTICLE INFO

*Article history:*
Received 6 July 2018
Received in revised form 18 September 2018
Accepted 28 September 2018
Available online 4 October 2018

Editor: Pavlos Kassomenos

*Keywords:*
Climate change
Heat wave
Cold wave
Extreme temperatures
Downscaling
Spain

## ABSTRACT

Heat- and cold-wave scenarios and temperature scenarios during the 21st century were obtained for Aragón (Spain), using, for the first time, nine Earth System Models (ESM) and two Representative Concentration Pathway (RCP) scenarios – RCP4.5 and RCP8.5 - belonging to the 5th Coupled Model Intercomparison Project (CMIP5).

Local climate heat-wave scenarios show an increase of its mean intensity close to 2 °C (reaching temperatures of up to 38.8 °C) and an average increase of the maximum intensity of 3.6 °C (temperature of up to 41.5 °C) with respect to a historic period (1971–2000) for the RCP8.5 scenario at the end of the century. The duration of heat waves will increase by 7 days at the end of the century (total average duration of 12 days). The future intensity and duration of cold-wave episodes will remain stable.

Local climate change scenarios for daily maximum temperatures show a gradual increase throughout the 21st century. The greatest increases will occur during the summer at the end of the century, reaching values of up to 7 °C for the RCP 8.5 scenario. The minimum temperature increases show similar behaviours to the maximum temperatures, but with less marked increases (3 °C and 5.6 °C for the RCP4.5 and RCP8.5 scenarios respectively in summer at the end of the century).

The highest temperatures and the intensity of the heat waves will be especially intense in the Ebro Valley, the most populated area. In addition, the Pyrenees will suffer the longest heat waves, especially at the end of the century, and the greatest increases in maximum temperatures.

The downscaling of the CMIP5 models, offers accurate scenarios -both spatially and temporally- of extreme temperatures and heat and cold waves, useful for decision-making for local adaptation to climate change but also as a reference for other European regions.

© 2018 Elsevier B.V. All rights reserved.

* Corresponding author at: Universidad San Jorge, Campus Universitario Villanueva de Gállego Autovía A-23 Zaragoza-Huesca, km. 510, 50830 Villanueva de Gállego, Zaragoza, Spain
*E-mail address:* rpino@usj.es (M.ªR. Pino-Otín).

https://doi.org/10.1016/j.scitotenv.2018.09.352
0048-9697/© 2018 Elsevier B.V. All rights reserved.

## 1. Introduction

There is widespread agreement in the scientific literature that the most severe effects of global warming will be related not only to a change in the mean climate, but especially to an increase in the frequency and intensity of extreme events, such as floods, droughts and heat waves as is reflected in the conclusions provided by the Intergovernmental Panel on Climate Change (IPCC) and in independent studies (Cook et al., 2013). Heat waves (i.e, a period of consecutive days with extreme hot temperatures) are one form of extreme weather that is likely to increase in frequency, intensity and duration under the influence of a changing climate during upcoming years (IPCC, 2013; Field et al., 2012). Extreme temperature events can impact many aspects of human life, such as mortality, health, comfort, agriculture and hydrology (Garcia-Herrera et al., 2005; Patz et al., 2005; Roldan et al., 2016). For example, in 2003, an extraordinary "mega heat wave" occurred in Central Europe, which had important consequences on society.

One of the main problems when evaluating extreme episodes of temperature (that is, cold or heat waves) is that there are no universal definitions of these phenomena. Some definitions use a fixed term (5 days >30 °C or 3 days >35 °C in the case of a heat wave); some include humidity, spatial extent or accumulated heat ((Anderson and Bell, 2009; Russo et al., 2017; Suparta and Yatim, 2017); some set their threshold according to a specific percentile (Anderson and Bell, 2009; Kent et al., 2014; Smith et al., 2013); and some are based on combined indexes of different meteorological variables, such as World Meteorological Organization member guidelines (WMO, 2010).

Although large-scale and small-scale processes involved in the development of European heat waves, such as interactions between land surface and atmosphere and the influence of large-scale atmospheric circulation, are not fully understood (Vautard et al., 2013), climate models could be a suitable tool for providing accurate heat-wave assessments for future adaptation strategies.

Global climate models (GCMs) are fundamental tools for the study of future climate, and they are able to provide data to estimate large-scale aspects of climate change, to drive regional climate models or to be used directly by impact models. GCM outputs are also used for projections of temperature extremes around the world (Dosio, 2017; Gross et al., 2017; Jeong et al., 2016; Saeed et al., 2017; Sillmann et al., 2014).

Recently, efforts to reduce model uncertainty have led to a new generation of global climate models called Earth System Models (ESM) that integrate the individual parts of the climate system (atmosphere, ocean, land and sea ice) and the exchange of energy and mass between them (Knutti and Sedlacek, 2013). They also include chemical processes, land use, plant and ocean ecology and an interactive carbon cycle, which enables integration of biochemical processes into the models (Heavens et al., 2013). These models are the basis of the fifth phase of the Coupled Model Intercomparison Project (CMIP5) (Taylor et al., 2012), constituting the most current set of coordinated climate model experiments (Brands et al., 2013; Carvalho et al., 2017; Chen et al., 2016; Perez et al., 2014).

The CMIP5 models and their predecessors have become an important resource for climate scientists and others investigating possible future impacts. However, the spatial resolution of these models remains too low for many impact assessments at a local scale, on which policy and management decisions need to be made. These models are run at coarse spatial resolutions, which is also a major limitation in projecting extreme events because projections of climate extremes and simulations of heat-wave characteristics on regional scales are very sensitive to spatial resolution and the interpretation of gridded outputs (Chen et al., 2016).

The deficiency in scale is addressed through downscaling techniques involving either statistical approaches or dynamic approaches. In the statistical approach, high-resolution predictands (surface variables) are obtained by applying relationships that are identified from the observed climate data to these predictands and to large-scale predictors of GCM outputs (Asong et al., 2016; Benestad et al., 2007; Semenov and Stratonovitch, 2010). In dynamical downscaling, a time-varying regional climate model (RCM) of atmospheric boundary conditions is nested within the GCM (Giorgi and Gutowski, 2015; Giorgi and Mearns, 1991;). Both methods have been widely used and both have advantages and disadvantages. The main advantages of statistical downscaling techniques are that they are computationally inexpensive, they provide local information and they allow quantifying the uncertainty associated to the downscaling process and to the climatic models.

Several studies have been carried out to explore present temperature extremes in Europe (Soares et al., 2012) and in the Mediterranean region (Kuglitsch et al., 2010; Seubert et al., 2014), and other studies have developed scenarios of temperature extremes in the same areas (Estrella and Menzel, 2013; Hertig et al., 2010; Lavaysse et al., 2012). However, none of them have applied the downscaling CMIP5 models.

Although many climate models have difficulties in properly reproducing climate extremes, such as heat-wave conditions (Stegehuis et al., 2015), a few studies have reported on heat-wave scenarios in Europe (Fischer and Schar, 2010; Schoetter et al., 2015), or located in in the Mediterranian region (Zittis et al., 2016), in France (Planton et al., 2008), Italy (Tomozeiu et al., 2007) or Finland (Kim et al., 2018). Schoetter et al. (2015) and Kim et al. (2018) are one of the few studies that already use the models from the IPPC5. As a part of the European Coordinated Regional Downscaling Experiment (EUROCORDEX) (Giorgi et al., 2009), the EUROCORDEX initiative provides regional climate projections for Europe. (Vautard et al., 2013) used the EUROCORDEX project to simulate heat waves at the European regional scale, providing a downscaling of CMIP5 simulations. These European-scale studies only featured a few locations in Spain. Several downscaling studies have been specifically conducted on temperature in Spain (Brands et al., 2011b; Frias et al., 2005; Frias et al., 2010; Hervada-Sala et al., 2000; Miro et al., 2016; Turco et al., 2014), but very few studies have explored temperature extremes in Spain (Fernandez-Montes and Rodrigo, 2012; Fonseca et al., 2016) and they do it in past periods (1925–2006 and 1986–2005, respectively).

Only a few studies have developed temperature scenarios in the Aragón region (northeastern Spain) (Buerger et al., 2007; Goncalves et al., 2014; Ribalaygua et al., 2013a), but none of them developed temperature-extreme or heat-wave scenarios. Only (Barrera-Escoda et al., 2014) developed scenarios of extreme temperatures in the Ebro basin. That study showed that the projected increase in the number of tropical nights and extreme temperatures could have a negative effect on human health and comfort conditions. Other studies have also analysed the possible impacts of climate change in this region on human health (Roldan et al., 2016). Both studies used the climate models associated to the 4th assessment report of the IPCC.

Aragón is characterised by a highly complex topography that causes large climate gradients. Downscaling techniques were required to capture these orographic features, allowing for the areas that were most vulnerable to extreme changes to be identified. Statistical downscaling is particularly recommended for areas with complex topography (Kattenberg and Amer Meteorol SOC, 1996). Nevertheless, downscaling of CMIP5 simulations has not been used to date, and heat-wave scenarios cannot be found in this sensible area of Spain.

Therefore, the objectives of this study were:

- Generate local heat- and cold-wave scenarios of the 21st century to downscale GCMs from CMIP5 using a statistical methodology in the area of Aragón, Spain.
- In addition, generate new climate scenarios using CMIP5 models for Aragón to simulate the future daily maximum and minimum temperatures in order to analyse the differences with respect to the scenarios we generated in 2013 for the 21st century using the Special Report on Emissions Scenarios, SRES (IPCC, 2000) previous to CMIP5.

Aragón, moreover, is a representative territory of different European climates, from the low-land areas in the centre of Aragón (the Ebro

River Basin) to the mountain regions in the north (the Pyrenees) which makes it a good indicator of future European climate changes. Finally, an original two-step analogue/regression statistical downscaling method developed by the Climate Research Foundation was carried out.

The information used in the present study was based on the most current data available. It was useful for identifying the areas that were most vulnerable to extreme temperature changes in Aragón, and for helping decision makers to design mitigation and adaptation strategies in response to territorial environmental impacts derived from climate change.

## 2. Material and methods

### 2.1. Study area and datasets

#### 2.1.1. Study area

The present study was carried out in the region of Aragón (Fig. 1), which is located in the northeast part of the Iberian Peninsula in Spain and which has an area of approximately 47,720 km$^2$ (340 km length and 240 km width). Because of its location, Aragón falls within the Western Mediterranean climate area, with cool winters and hot, dry summers. However, the extreme altitude differences of over 3000 m between the plains (the Ebro River Basin) and the mountains (the Pyrenees), together with the specific topography of the Ebro River Basin and the mountain chains (the Pyrenees to the north of the basin and the Iberian Mountains to the south), modify the local climate. As a result, the climate characteristics of the area are somewhat different from a standard Western Mediterranean climate, and they typically consist of dryness of the land along the banks of the Ebro River, random rain patterns, high thermal contrast between winter and summer as a consequence of the strong continental characteristics of the region and the typical northeast "mistral" winds, which are frequent in the region.

#### 2.1.2. Surface observation dataset (predictands)

The observational dataset used in the present study consists of a time series of the daily maximum and minimum temperatures distributed, quite homogeneously, throughout the Aragón territory (Fig. 1). This dataset it is the same as the one used in a previous study (Ribalaygua et al., 2013a) in order to facilitate comparison of the results.

Data were obtained from the extensive network of instrumental observatories owned by the Spanish Meteorological Agency (AEMET) (http://www.aemet.es). The stations are subject to strict data quality control, which includes detecting and correcting multiple aberrant points in the long-term climate time series, covering the gaps, assessing the homogeneity of the climate series and correcting any inhomogeneities found. This process was carried out by the Aragón Government (López et al., 2007) To guarantee the quality of the data, stations with a large number of data gaps or without at least 15 years of daily records were discarded. Second, we analysed the dataset for the presence of extreme data points that could be considered suspect observations or transcription errors (we considered data points to be extreme if they were separated from the monthly average by more than four times the value of the standard deviation). Third, we verified that the data did not contain inhomogeneities that could introduce bias into any records that were not related to the climate, (Ribalaygua et al., 2013a).

The first set of data (composed of 103 stations) was used to analyse and produce the regional climate scenarios of maximum and minimum temperatures (Fig. 1a). Of these 103 stations, those that had at least 75% of maximum temperature data collected from June to September (i.e, the reference period for the calculation of heat waves) between 1980 and 2000 and stations that had at least 75% of minimum temperature data collected from November to April (that is, the reference period for the calculation of cold waves) between 1980 and 2000 perform a second set of data selected for the study of extreme events. In both cases, the number of observatories was 71 (Fig. 1b).

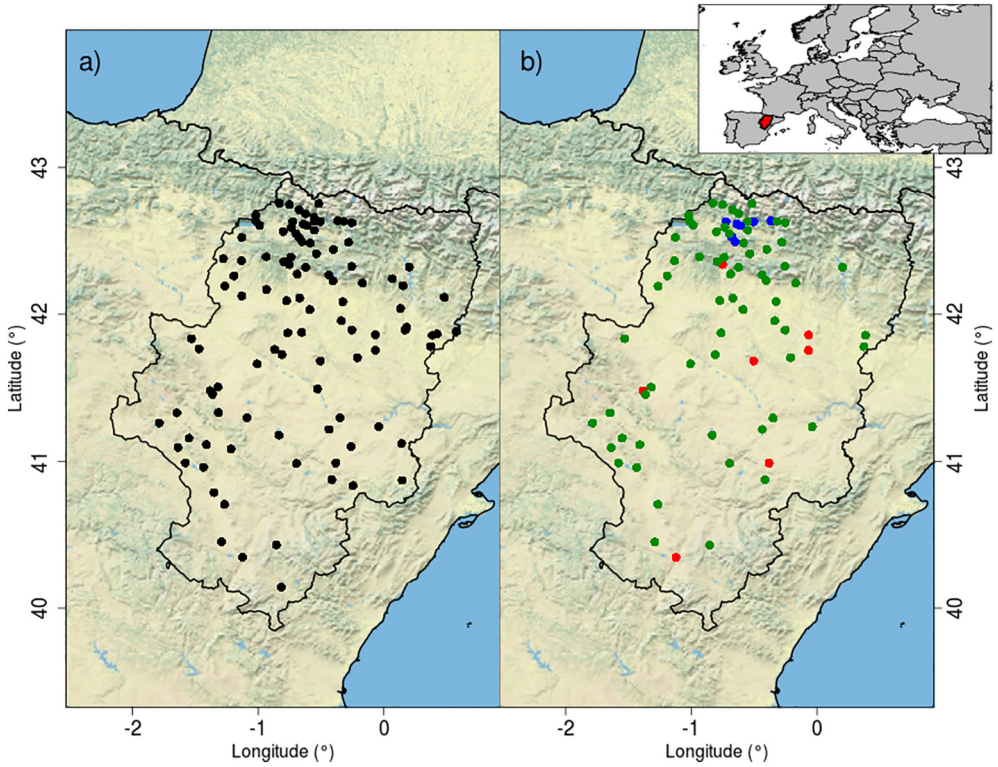


**Fig. 1.** Location of the study Area: Aragon (Spain) in Europe. Points indicate the stations used in the study. a) Stations of temperature (103) used in the generation of climate regional scenarios of maximum and minimum temperature (verification, validation and scenarios). b) Stations used exclusively on the generation of heat waves (7, red), used exclusively on the generation of cold waves (7, blue) and those used in both extreme events (64, green). "(Map source: OpenStreetMap)".

*2.1.3. Atmospheric dataset (predictors)*

*2.1.3.1. Reanalysis.* As a reference dataset, we used the reanalysis from the European Centre for Medium-Range Weather Forecasts (ECMWF ERA-40; http://www.ecmwf.int/research/era/do/get/era-40) (Uppala et al., 2005) for the period 1958–2000. For the atmospheric window, we used geographical limits from 31.5°N to 55.1°N latitude and from 27.0°W to 14.6°E longitude, covering not only the geographic area under study, but also the surrounding atmosphere areas, which exert a meteorological influence all over the Iberian Peninsula (Ribalaygua et al., 2013a).

For verification of the methodology, it was necessary to reduce the temporal (six hourly) and spatial (125 km) scale of the reanalysis to that of the different climate models in order to compare both, ERA-40 and the climate model simulations (Ribalaygua et al., 2013a, 2013b).

*2.1.3.2. Climate model data.* In the present study, we worked with a set of nine climate models that belong to the CMIP5 and that were provided by the Program for Climate Model Diagnosis and Intercomparison (PCMDI) archives (Table 1). The number of models chosen was limited to the availability of data with daily time frequencies. All of the models were ESMs.

To generate the model predictor fields, we took the daily values of several large-scale fields of interest (that is, geopotential height, specific humidity and wind) at different pressure levels for the nine ESMs showed in the Table 1 associated with the CMIP5 (Taylor et al., 2012). Moreover, we used an historical experiment (Taylor et al., 2012) which generated simulations of the past 20th century and which was useful for the evaluation of model performance against the present climate. Finally, the representative concentration pathway (RCP) families were considered (Moss et al., 2010), specifically the RCP8.5 'high' scenario and the RCP4.5 'intermediate' scenario, both of which corresponded to different possible ranges of radiative forcing reached in the year 2100 with respect to values of the pre-industrial era (4.5 and 8.5 W/m$^2$, respectively).

*2.2. Methodologies*

*2.2.1. Description of the downscaling methodology*

The methodology of statistical downscaling used in this study was chosen according to three main advantages:

1) Allows easier quantification of the main uncertainties associated with the generation of future climate scenarios (Van der Linden and Mitchell, 2009).
2) It is a key for the achievement of climate simulations that are consistent with observations which, in turn, are physically coherent (Ribalaygua et al., 2013b).
3) Provides local detail, which is useful information because nearby data points in space can evolve under different future climate conditions (Ribalaygua et al., 2013b).

A two-step analogue/regression statistical downscaling method that was developed by the Climate Research Foundation (FIC) (Ribalaygua et al., 2013b) was applied to obtain future scenarios of the maximum and minimum temperatures at a local scale in the region of Aragón. This methodology consisted of a two-step analogue/regression statistical method, which has been used in national and international projects with good verification results. In the present paper, we present a summary of the two-step method (more details can be found in Ribalaygua et al., 2013b).

The first step was analogous stratification. An analogue method was applied based on the hypothesis that 'analogue' atmospheric patterns (predictors) should cause analogue local effects (predictands), which means that the number of days that were most similar to the day to be downscaled were selected (Benestad et al., 2007; Zorita and von Storch, 1999). The similarity between any two days was measured using a pseudo-Euclidean distance between the large-scale fields used as predictors. For each predictor, the weighted Euclidean distance was calculated and standardised by substituting it with the closest percentile of a reference population of weighted Euclidean distances for that predictor. This method is a good method for reproducing nonlinear relationships between predictors and the predictands, but it could not be used to simulate values outside of the range of observed values ((Imbert and Benestad, 2005). In order to overcome this problem and to obtain a better simulation, a second step was required.

The second step focuses on temperature. To determine the temperature, a multiple linear regression analysis for the selected number of most analogous days was performed for each station and for each problem day. From a group of potential predictors, the linear regression selected those with the highest correlation, using a forward and backward stepwise approach.

About the accuracy in simulating temperatures of our downscaling technique, in our previous work about climate change in Aragón we achieved an average bias below 0.1 °C″ (Ribalaygua et al., 2013a).

**Table 1**
Information about the nine climate models belonged to the 5 Coupled Model Intercomparison Project (CMIP5) corresponding to the fifth report of the IPCC. Models were supplied by the Program for Climate Model Diagnosis and Intercomparison (PCMDI) archives.

| Climatic model | SPATIAL/TEMPORAL resolution | Research centre | References |
|---|---|---|---|
| GFDL-ESM2M | 2°×2,5° daily | National Oceanic and Atmospheric Administration (NOAA), E.E.U.U. | Dunne et al. (2012) |
| CanESM2 | 2,8°×2,8° daily | Canadian Centre for Climate Modeling and Analysis (CC-CMA), Canadá. | Chylek et al. (2011) |
| CNRM-CM5 | 1,4°×1,4° daily | CNRM (Centre National de Recherches Meteorologiques), Meteo-France, Francia. | Voldoire et al. (2013) |
| BCC-CSM1-1 | 1,4°×1,4° daily | Beijing Climate Center (BCC), China Meteorological Administration, China. | Xiao-Ge et al. (2013) |
| HADGEM2-CC | 1,87°×1,25° daily | Met Office Hadley Center, United Kingdom. | Collins et al. (2008) |
| MIROC-ESM-CHEM | 2,8°×2,8° daily | Japan Agency for marine-Earth Science and Technology (JAMSTEC), Atmosphere and Ocean Research Institute (AORI), and National Institute for Environmental Studies (NIES), Japan. | Watanabe et al. (2011) |
| MPI-ESM-MR | 1,8°×1,8° daily | Max-Planck Institute for Meteorology (MPI-M), Germany. | Raddatz et al. (2007); Marsland et al. (2003) |
| MRI-CGCM3 | 1,2°×1,2° daily | Meteorological Research Institute (MRI), Japan. | Yukimoto et al. (2011) |
| NorESM1-M | 2,5°×1,9° daily | Norwegian Climate Centre (NCC), Norway. | Bentsen et al. (2013); Iversen et al. (2013) |

*2.2.2. Validation and climate simulation of temperature*

In order to determine the ability of each ESM to simulate the predictor fields, absolute and relative temperatures from the downscaled ESM simulation of the historical experiment was compared with the downscaled ERA-40 simulation (previously verified against the observations) during a common historical period (1958–2000).

Due to the characteristics of the ESMs, the validation process presents certain limitations. First, as climate models do not reproduce day-to-day meteorology, validation cannot be performed on a daily scale and it must be done using climate statistics over long periods of time, resulting in a loss of information on climate variability. Second, we could not compare the climate characteristics obtained from the ESM historical simulation with those obtained from the observations because the latter had missing data and large gaps; therefore, we had to compare ESMs simulations with simulations from the re-anlaysis of a dataset (previously validated in the verification process). Both sources of error should be considered in the final uncertainty analysis.

As error measures, bias and standard deviation were analysed on a seasonal scale for both maximum and minimum temperatures. An ensemble strategy was used to quantify the uncertainties inherent in future climate projections (IPCC, 2013). For each scenario (i.e, RCP4.5 and RCP8.5), an ensemble of the approved downscaled ESMs was used to estimate the mean change (compared to 1976–2005) and to quantify the main contributions to the uncertainty.

Future local climate scenarios for maximum and minimum temperature, for nine GCMs and two RCPs have been produced at the daily scale. To draw the temperature maps, we used Thin Plate Spline regression (TPS) from the R-Package "fields" (Nychka et al., 2015).

*2.2.3. Definition of hot- and cold-wave episodes*

There are many and varied terms used to define a heat wave. For example, the AEMET defines a heat wave as an "episode of at least three consecutive days, in which at least 10% of the stations considered record maximums above the 95% percentile of their series of maxima daily temperatures of the months of July and August of the period 1971–2000." The WMO defines a heat wave as an extreme event with marked warmed of the air or the invasion of very warm air over a large area, it usually last from a few days to a few weeks. The IPCC defines a heat wave as "a period [of] abnormally and uncomfortably hot weather". Those definitions are not the only ones accepted in the

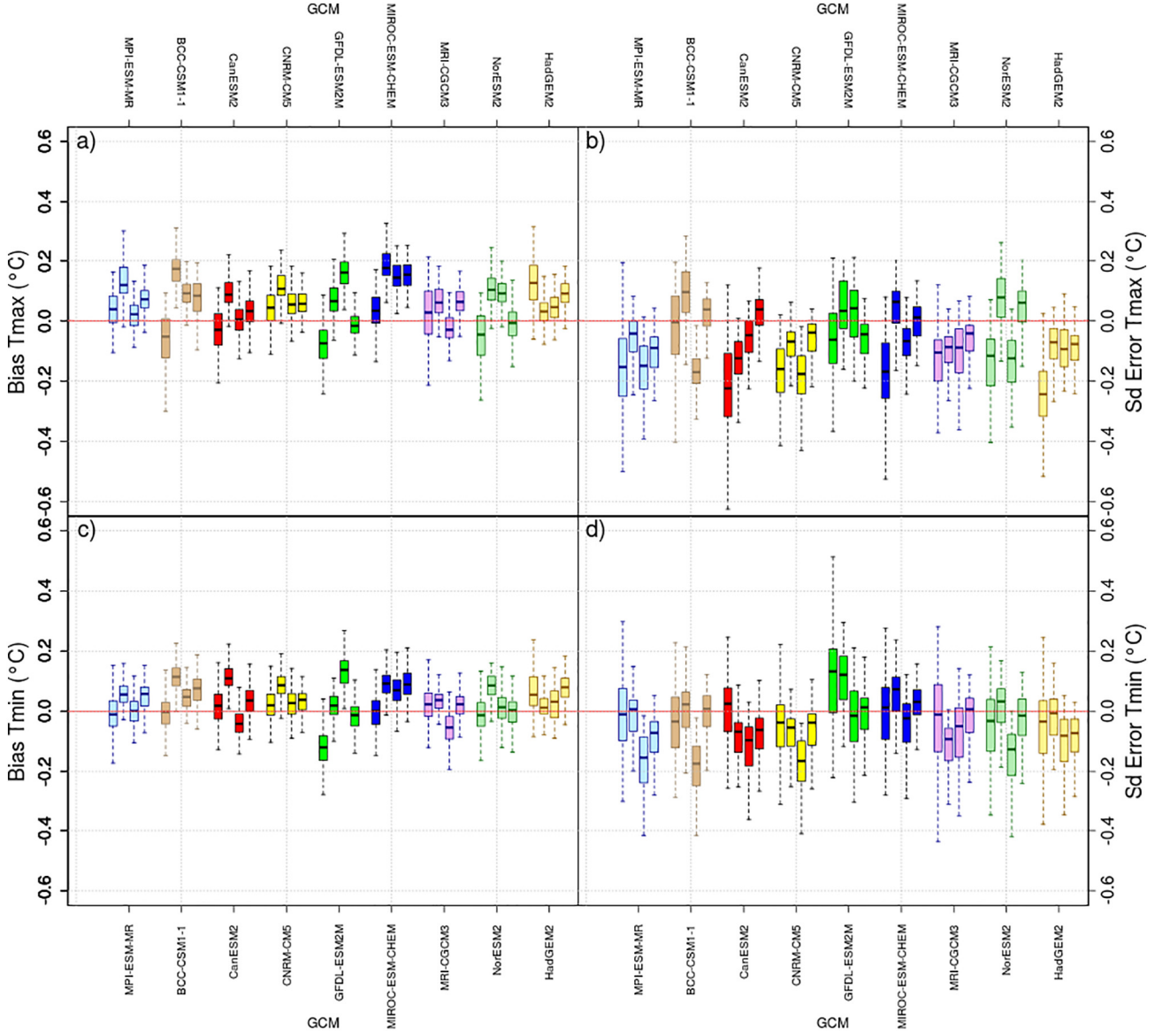


**Fig. 2.** Validation of the GCMs used for the simulation of temperatures. Absolute Bias for a) maximum and c) minimum temperature and absolute standard deviations for b) maximum and d) minimum temperature, between the results obtained by downscaling the Historical scenario of each GCM used in the study with those obtained by downscaling the reanalysis ERA-40 for a common period (1958–2000). There are four boxplots, representing a season of the year (winter, spring, summer and autumn), for each GCM.

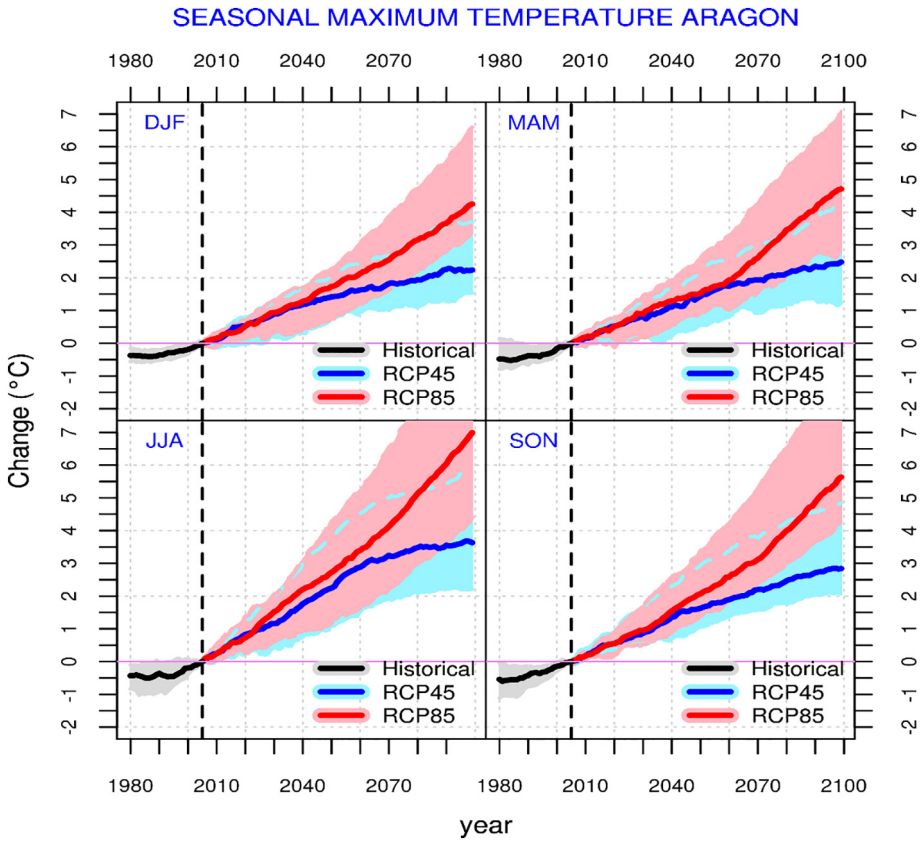


**Fig. 3.** For the four seasons (winter, spring, summer and autumn) simulated maximum temperature for the twenty-first century displayed as absolute increase against the value simulated for the 1976–2005 Historical period. The vertical dotted line marks the end of the Historical data (2005). Data grouped for every RCP simulation of every global climate model used and for the last 30 years of every station. The ensemble median (solid lines) and the 10th–90th percentile (shaded areas) values are displayed.

scientific literature. Some heat-wave definitions have been used to identify heat waves in a time series of temperature data (Smith et al., 2013;), and the choice of the heat wave definition can influence both projected heat-wave trends (Smith et al., 2013) and estimates of health risks during events (Anderson and Bell, 2009; Chen et al., 2015; Kent et al., 2014).

According to the recommendations of the WMO, (2010), a practical and qualitative definition of a heat wave must consider marked and unusual hot weather over a region during at least two consecutive days in the hot period of the year, based on local climate conditions, with thermal conditions recorded above given thresholds. On the basis of these recommendations and the characteristics of the Aragón climatology, we defined a heat wave as follows: at least three consecutive days with a maximum temperature above the 95th percentile of the maximum temperature series and calculated between the months of June to September during the period 1980–2000.

In broad terms, a cold wave can be defined as a meteorological event characterised by a sharp drop of air temperature near the surface, leading to extremely low values. According to the IPCC 2007, (Parry et al., 2007) a cold wave is an event that often causes problems and severe impacts on the population, especially in northern altitudes. However, there is still a lack of a clear and consistent definition for cold-wave events in the world.

In the WMO's Meteoterm vocabulary, a cold wave is defined as "marked cooling of the air, or the invasion of very cold air, over a large area." For the AEMET, a cold wave is "an episode of at least three consecutive days, in which at least 10% of the considered stations register minimums below the 5% percentile of their series of minima daily temperatures for the months of January and February of the period 1971–2000". The WMO's members guideline define a cold wave as "marked and unusual cold weather characterised by a sharp and significant drop of air temperatures near the surface (max, min and daily average) over a large area and persisting below certain thresholds for at least two consecutive days during the cold season".

Considering the climate characteristics of Aragón, we defined a cold wave as follows: at least three consecutive days with a minimum temperature below the fifth percentile of a minimum temperature series and calculated between the months of November to April during the period 1980–2000.

To better identify a heat or cold wave, we evaluated average duration, maximum intensity and average intensity as it is recommended by the WMO in the Guidelines on the definition and monitoring of extreme weather and Climate Events. The average duration refers to the average number of days the heat wave lasted. The average intensity represents the average value of the temperature during the heat wave. The maximum intensity is equal to the maximum value that the temperature reached during the heat wave.

*2.2.4. Verification and simulation of heat and cold waves*

In order to assess the capacity of the downscaling methodology to simulate heat and cold waves observed in the past, we evaluated how the downscaling methodology simulated the 95th percentile of maximum temperatures and the 5th percentile of minimum temperatures, which are the thresholds that indicate the existence of an episode of a heat and cold wave, respectively. In addition, we analysed the intensity of the wave (average and maximum) and the average duration, comparing the heat and cold waves calculated from the simulated ERA-40 temperature series with those obtained from the observed series. Verification of the maximum and minimum temperatures can be seen in a previous study by Ribalaygua et al. (2013a). The statistical measures used in the verification processes were the bias, the standard deviation and the Pearson correlation at the daily scale. The statistical

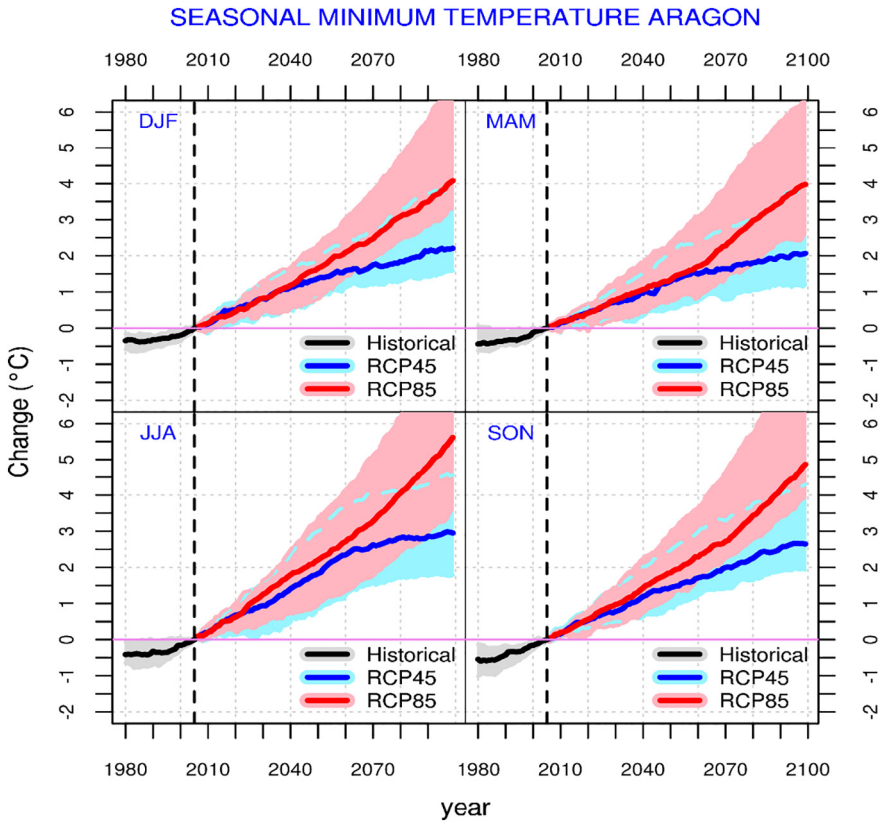


**Fig. 4.** For the four seasons (winter, spring, summer and autumn) simulated minimum temperature for the twenty-first century displayed as absolute increase against the value simulated for the 1976–2005 Historical period. The vertical dotted line marks the end of the Historical data (2005). Data grouped for every RCP simulation of every global climate model used and for the last 30 years of every station. The ensemble median (solid lines) and the 10th–90th percentile (shaded areas) values are displayed.

measures were calculated using R-cran package computing software (R Development Core Team, 2010).

From the ESM simulated temperature series (nine ESMs and two RCPs), we determined the heat- and cold-wave episodes that were expected in Aragón during the upcoming decades of the 21st century. The heat- and cold-wave scenarios were compared to a historical period (1976–2005) to analyse the future changes with respect to the actual situation of these extreme events.

## 3. Results

### *3.1. Validation of the CMIP5 model statistical downscaling to predict temperatures*

The seasonal bias that result from a comparison between the ERA-40 temperature simulations and the historical temperature simulations for each ESM for a common period (1958–2000) are shown in Fig. 2 for absolute temperatures (that is, the difference between simulated Historical ESM data and simulated ERA-40 data). For both the maximum and minimum temperatures, the obtained bias was around tenths of a degree in all months, so they were very close to zero. The error was not above half of a degree for any of the cases. Therefore, the results showed that the ESMs were capable of adequately simulating both the maximum and the minimum temperatures on annual and seasonal scales.

### *3.2. Local climate scenarios to predict future temperatures*

Figs. 3 and 4 show local climate-change scenarios for future daily maximum and minimum temperatures respectively, that have been predicted on the basis of the nine models (see Table 1). Figs. 3 and 4 allowed for the establishment of a general view of the changes expected in Aragón. In addition, Figs. 5 and 6 represent the summer maximum and winter minimum temperature changes expected for the periods 2041–2070 and 2071–2100 as presentation of mid- and end-century expected changes, which were calculated according to the scenarios RCP4.5 and RCP8.5.

Expected changes in the average temperature for the rest of the seasons of the year can be found in the supplementary material for maximum temperatures increase (Figs. S1–S3) and minimum temperatures increase (Fig. S4–S6). In addition, Fig. S7–S9 showed the maximum and Figs. S10–S12, minimum temperatures expected in this century.

Fig. 3 shows a gradual increase in the maximum temperatures throughout the 21st century. During the mid-century, the least significant changes are expected during the winter and springs months (around 1.5 and 1.7 °C for the RCP4.5 and RCP8.5, respectively), and the most significant changes are expected for the summer months, with values of 2.1 °C for the RCP4.5 and 2.7 °C for the RCP8.5. At the end of the century, the expected changes are more marked and differ notably between the two RCPs. During winter and spring months, the expected values are around 2.3 °C and 2.4 °C for the RPC4.5 and 4.3 °C and 4.7 °C for the RCP8.5, respectively. The greatest changes are expected for summer months, reaching values of 7 °C for the RCP8.5 and 3.6 °C for the RCP4.5.

The areas most affected by the maximum temperature increases are expected to be the Pyrenees and the areas in the southwest and north of Aragón during all the 21th century for the months of summer, spring and autumn, especially in the RCP8.5 scenario (Fig. 5). In contrast, in the winter months, the highest temperature increases at the end of the century are expected in the Pyrenees area and the Ebro Valley (Fig. S1).

Scenarios of maximum temperatures of the 21st century (Figs. 5 and S7–S9) point that expected maximum temperatures are not proportional to the expected increases shown before (Figs. 5 and S1–S3).

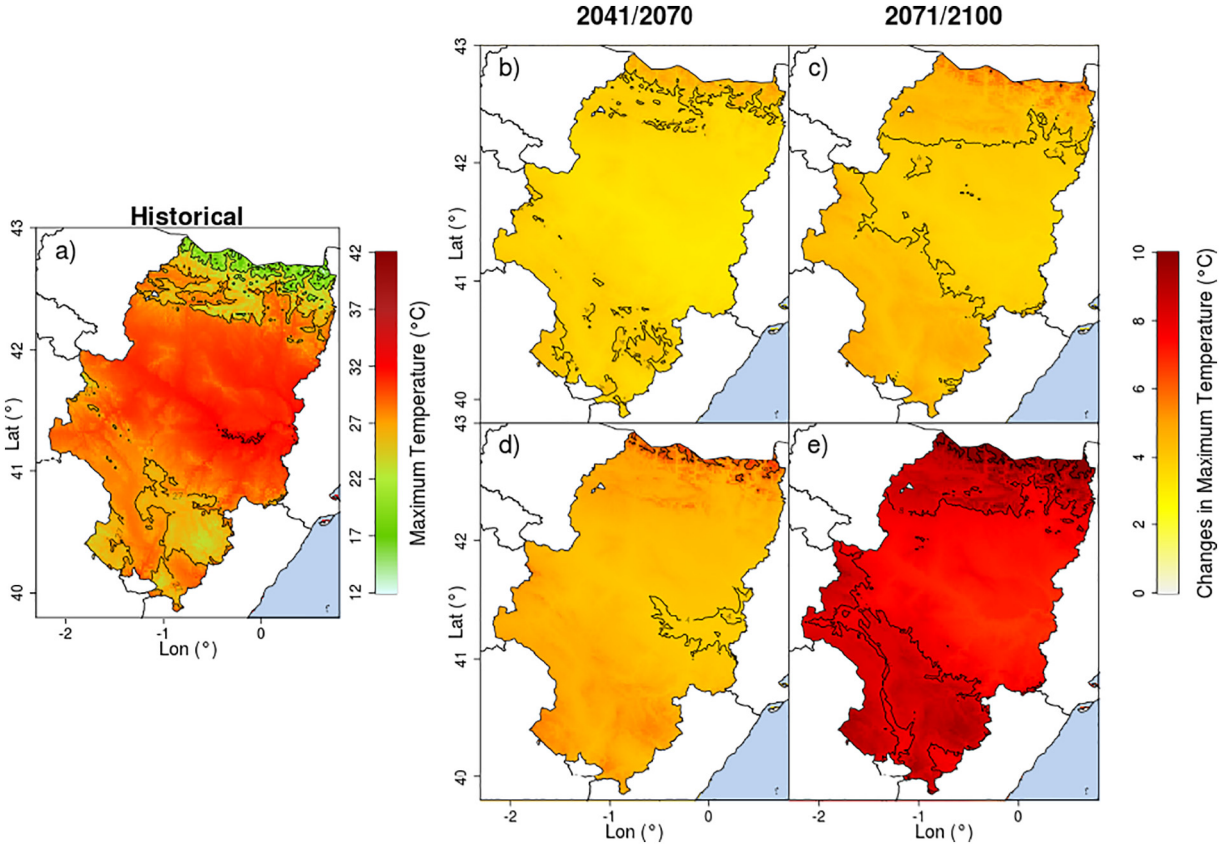


**Fig. 5.** Geographical representation of the expected changes of maximum temperature in summer for the periods 2041–2070 and 2071–2100 respect to the reference Historical Period (1976–2005). Both emissions scenarios are represented: RCP4.5 (figures b and c) and RCP8.5 (figures d and e). Fig. 5a represents the Historical absolute temperature for the period 1976–2005.

The evolution of the minimum temperature increases throughout the 21st century demonstrate similar behaviours to the maximum temperatures, but with less marked increases, especially at the end of the century (Figs. 6 and S4–S6). By the middle of the century, all of the seasons of the year, except for the summer, are expected to show increases in the minimum temperature of <2.0 °C, and even in the spring, the increases are expected to be close to 1.0–1.2 °C. The summer months are expected to show the greatest increases in minimum temperatures, varying from 1.8 °C for the RCP4.5 to 2.3 °C for the RCP8.5. At the end of the century, increases in the minimum temperatures during the summer months are expected to range from 3.0 °C (RCP4.5) to 5.6 °C (RCP8.5. Winter months are expected to show an increase between 2.8 °C and 4.1 °C, spring months between 2.1 °C and 4 °C and autumn months between 2.6 °C and 5 °C for the RCP4.5 and RCP8.5 scenarios, respectively.

The increases in the minimum temperature in are expected to be quite homogeneous throughout the region and the seasons according to the RCP4.5. In contrast, according to RCP8.5 (Fig. 6c,d), these changes will be more pronounced in the Ebro Valley at the end of the 21st century. The highest minimum temperatures are expected to be recorded in the central zone of Aragón during all seasons of the year (see supporting information, Figs. S10–S12).

### 3.3. Verification of hot- and cold-wave episodes

To verify the simulation of both of heat waves and cold waves, we compared the wave episodes obtained from ERA-40 simulations against the episodes recorded by the observations.

The first step was to verify that the methodology correctly simulated both percentiles, the 95th percentile of the maximum temperature and the 5th percentile of the minimum temperature. Both cases have been well simulated by applying the downscaling methodology to the ERA-40 series (Fig. 7). Data from the simulated ERA-40 series and the observed series were very close, and the error committed by simulating the ERA-40 series respect to the observed one was very low, especially in the 95th percentile. For example, we found error values around 0.36 °C for summer months and around 0.69 °C for the winter months in the 95th percentile, and 0.6 °C for summer months and around 0.68 °C for the winter months in the 5th percentile.

Regarding the verification of the identification parameters of a heat wave, Fig. 8 shows the results obtained for the duration of a heat wave, its temporary occurrence and its average intensity (maximum intensity is not shown here, but it was also taken into account in the present study and can be seen in Support Information (S13)).

As can be seen in Fig. 8a and b the average intensity of observed heat waves and ERA-40 simulations are very similar in the 71 observatories. We found a high correlation between the average intensity of a heat wave and the results from the observed and the simulated ERA-40 scenarios ($p = 0.9889$). A similarly high correlation was obtained in terms of the maximum intensity of a heat wave ($p = 0.9883$, not shown here).

Regarding to the average duration of heat waves episodes, Fig. 8c and d showed a similar pattern of temporal and spatial distribution and a strong correlation ($p = 0.8976$). For example, both datasets showed a clear signal of heat waves during the years 1982, 1987, 1990, 1994 and 1998, and they both showed no heat wave during the years 1986, 1987, 1996 and 1997.

Similar results are present in Fig. 9 for cold waves. In this case, the correlation obtained between the average duration of the observed cold waves (Fig. 9c) and those simulated for ERA-40 (Fig. 9d) was $p = 0.8593$, which was lower than the p-value obtained for heat waves. The correlations of the intensities between both groups of data were strong ($p = 0.8849$ and $p = 0.792$ for maximum intensity and average

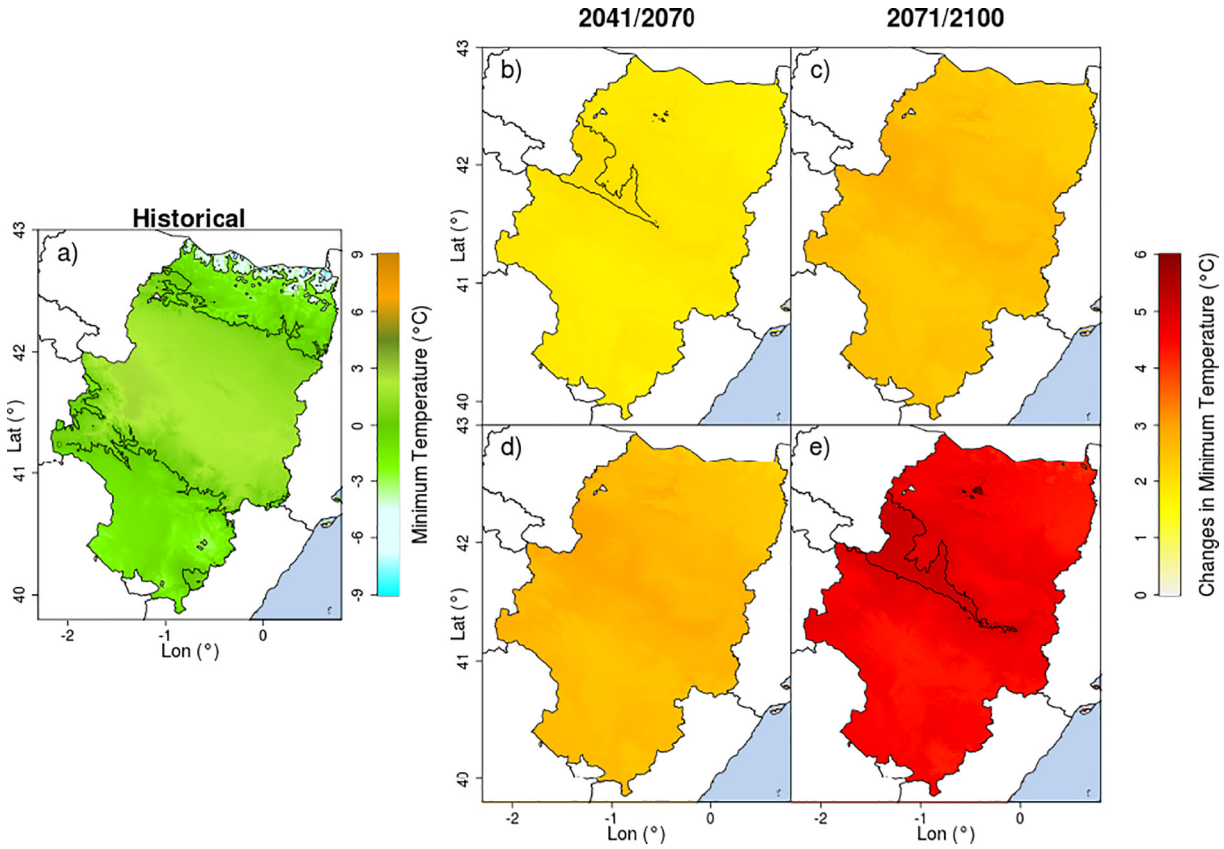


**Fig. 6.** Geographical representation of the expected changes of minimum temperature in winter for the periods 2041–2070 and 2071–2100 respect to the reference Historical Period (1976–2005). Both emissions scenarios are represented: RCP4.5 (up, figures b and c and RCP8.5 (figures d and e). Panel a represents the Historical absolute temperature for the period 1976–2005.

intensity, respectively), but lower than those obtained for the heat waves. The cold-wave pattern (that is, duration, average intensities and maximum intensities) were very similar in both datasets, marking episodes of cold waves during the same time periods.

### *3.4. Local future climate scenarios of hot- and cold-waves episodes*

Figs. 10 and 11 show the climate scenarios for heat waves in Aragón according to the RCP4.5 and the RCP8.5scenarios, respectively. The figures show the temporal evolution (from historical data to 2100) for three main features of the heat waves: average intensity (first row), maximum intensity (second row) and average duration (third row). The temporal periods analysed were 1976–2005 (historical; first column), 2041–2070 (second column) and 2071–2100 (third column). These periods were chosen as representative of the present, mid-century and end-century periods. Figs. 12 and 13 show the same information but for cold waves.

In addition, in Support information heat and cold waves are represented as increments in temperature for heat waves (S15 and S16 for RCP4.5 and the RCP8.5 scenarios, respectively) and for cold waves (S17 and S18 for RCP4.5 and the RCP8.5 scenarios, respectively).

During the coming decades, an increase in the duration of heat waves is expected. According to the RPC4.5, sharp increases in the average intensity of heat waves are not expected with respect to the values corresponding to the historical period (an average of approximately 0.8 °C). This means that a mean intensity of 37.6 °C is expected at mid-century and 37.8 °C at the end of the century. According to the RCP8.5, the average intensity would increase an average of approximately 1–1.2 °C during the middle of the century (reaching 38 °C) and close to 2 °C at the end of the century (reaching 38.8 °C).

In the case of the maximum intensity of the heat waves, the average increases with respect to the expected historical period were somewhat more pronounced than those expected for the average intensity, especially in the case of RCP8.5. According to RCP4.5, average increases of 1.4 °C and 1.7 °C (reaching 39.3 °C and 39.6 °C) are expected in the maximum intensity during the middle and end of the century, respectively. In the case of RCP8.5, those average increases are expected to rise to 2 °C and 3.6 °C (reaching 39.9 °C and 41.5 °C) during the middle and end of the century, respectively.

Note that for the average (maximum) intensity, there was a difference between observatories, such that in some of them the intensity could reach 46 °C (48 °C), while in other parts of the region it would not exceed 32 °C (34 °C) according to the RCP8.5.

The average and maximum intensity of the heat waves will be especially intense in the Ebro Valley in the middle of the century, and it will spread throughout the entire territory toward the end of the century, except for the Pyrenean area further north.

According to RCP4.5, an average increase in the number of days that lasts a heat waves (duration) compared to the historical period of about 2 days is expected during mid-century (2041–2070), with a maximum increase of 11 days, which would mean that the average duration of heat waves it would be around 7 days, with durations that vary between 4 and 18 days according to the station. At the end of the century, very sharp variations are not expected with respect to half a century. Results from the RCP8.5 predict that the average duration of heat waves will increase by 3 days in the middle of the century and by 7 days at the end of the century, which means that heat waves would have an average duration of between 8 and 12 days, respectively. Note that according to the RCP8.5 scenario, some observatories are expected to experience sharp increases during the historic period of up to 16 and 44 days for the period 2041–2070 and 2071–2100 respectively, so there would be

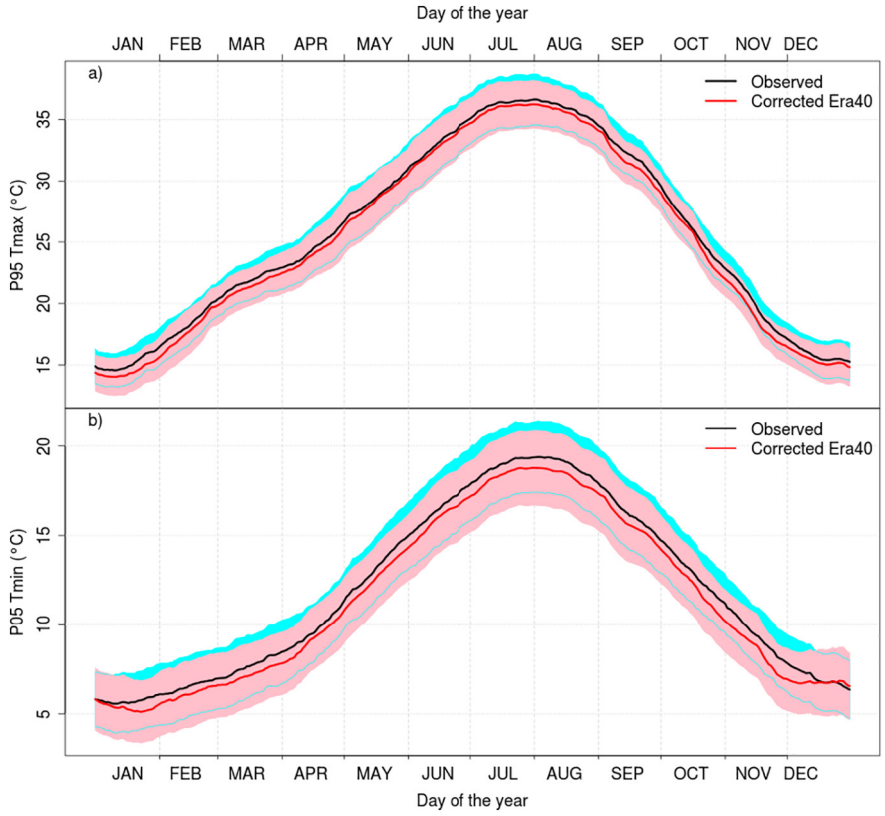


**Fig. 7.** Results of the verification process obtained for a) the 95th percentile of maximum temperature and b) the 05th percentile of minimum temperature comparing the results obtained by downscaling the reanalysis ERA-40 (black) along the observations (red) for a common (1980–2000). The solid lines represent the median and the shaded areas the 10-90th percentile of the values.

observatories where the consecutive days that exceed the "hot-day" threshold would be 23 and 52 days, for the same periods.

In this case, the Pyrenees to the north and the Iberian to the south of Aragón are the zones that would suffer longer heat waves; although, as we have seen, they would be the least affected by the intensity of the expected heat waves.

On the other hand, the episodes of cold waves would not change either the average or maximum intensity values (see Figs. 12 and S17 for the RCP4.5 scenario and Figs. 13 and S18 for the RCP8.5). The variations of average intensity with respect to the historic period are, on average, ±0.5 °C, and in some observatories they could reach ±1.0–1.°5 °C, independent of the RCP.

A similar pattern is expected for the maximum intensity of the cold waves (Figs. 12b and 13b), with few variations with respect to the historical period and similar patterns to those expected for the mean intensity. The north and the south of the territory are the regions that are expected to be the most affected by the intensity of the cold waves.

During the upcoming decades, an increase in the duration of cold-wave episodes is not expected. Both RCP4.5 (Figs. 12h and S17h) and RCP8.5 (Figs. 13h and S18h) predict that by the middle of the century, the average duration of cold waves will remain around 4 to 5 days, with episodes of 3 to 7 days in the middle of the century and 11 days at the end of the century. This would mean that the average duration of cold waves would not be modified with respect to the historical period, unlike what is expected in the case of heat waves, and in the most severe cases, the increase would be about three days at the end of the century. No differences of this pattern are expected in the territory.

## 4. Discussion

In the present study, heat- and cold-wave scenarios for the 21st century were obtained for the first time in the region of Aragón, Spain, using new ESMs belonging to the CMIP5. In addition, the climate scenarios for temperatures in this region were reconstructed with the new ESMs in order to assess differences with respect to the models used prior to CMIP5. These results offer one of the best snapshots of future climate change based on currently available data on the risks that extreme temperatures can cause in the Aragón region, both spatially and temporally.

### *4.1. Considerations of the temperature scenarios*

The new models used in the present study to obtain climate scenarios in Aragón are ESMs, not climate models. The improvements incorporated in the ESMs allow for greater precision in the simulation of climate variables, which provides evidence that the results of the validation are good.

The validation of the ESMs was good for both maximum and minimum temperatures. The differences between seasonal means were practically negligible (below a few tenths of a degree in temperature), and the differences between seasonal standard deviations were almost always below the reference values for every ESM (the standard deviation of the downscaled reanalysis data).

The validation results obtained in the present study show lower error rates than those obtained by the scenarios described in the fourth IPCC report and presented in previous studies (Ribalaygua et al., 2013a). In that case, the error was 1 °C, and even in some models (for example, the CNCM3 model in the summer), it was around 1.5 °C; in contrast, the results presented here did not reach such high values. Likewise, the values of the standard deviation are lower than those obtained in the previous study (5–10% in the present study vs 15–20% in a previous study (Ribalaygua et al., 2013a).

Another key point that justifies the generation of new climate scenarios for Aragón is the current designation of climate scenarios

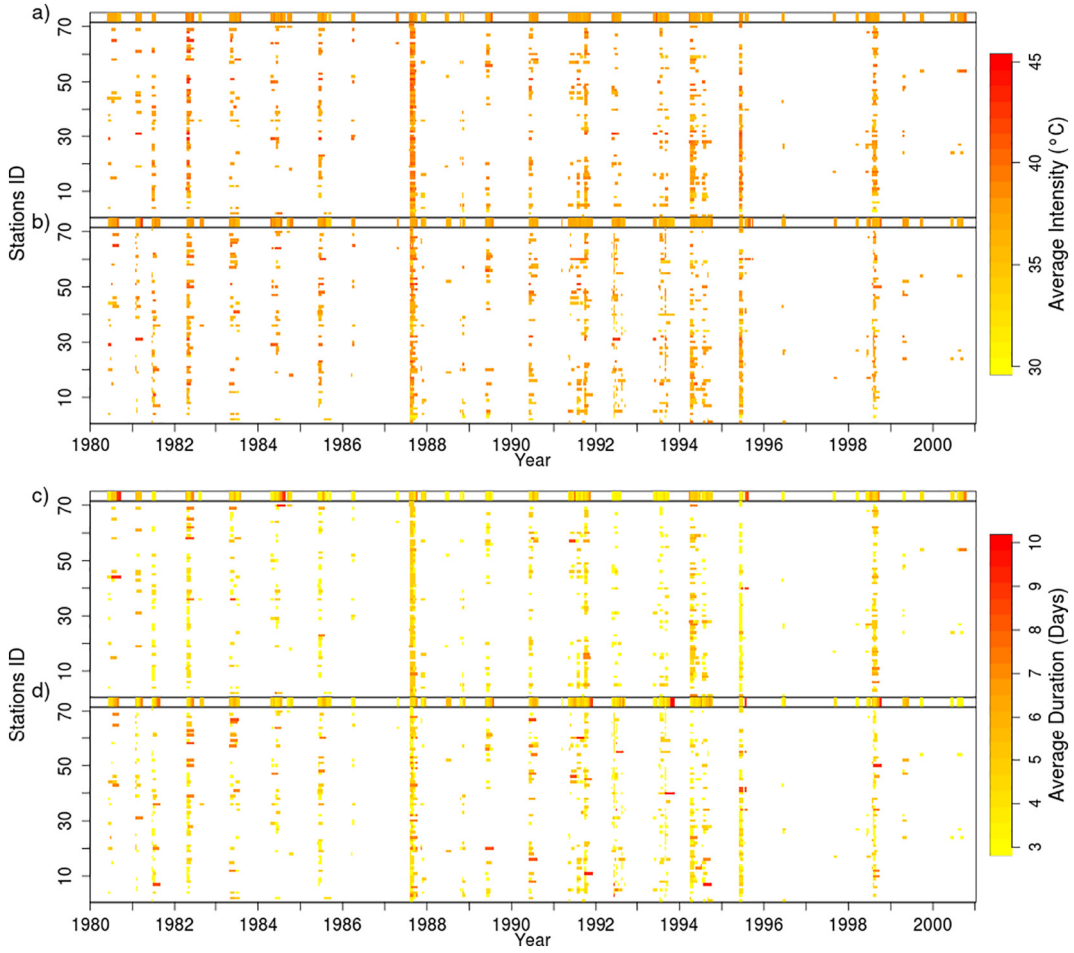


**Fig. 8.** Results of the verification process for heat waves obtained comparing the simulated heat waves for the reanalysis Era40 along the observed heat waves for a common period (1980–2000). a) Average intensity of the heat waves registered in the 71 stations used in the study against b) the average intensity obtained by downscaling of the reanalysis ERA-40 in these stations for the period 1980–2000. The colour of each pixel shows the average intensity that corresponds to each heat wave (°C), each column represents one year of the considered period and each row one station The upper row shows the mean of the average intensity from the whole observatories. Down, c) and d) same as a) and b) but for the duration of the heat waves. The colour of each pixel shows the duration corresponding to each heat wave (number of days).

provided by IPCC experts—that is, RCPs. Therefore, obtaining local climate scenarios that are based on the most current information is a priority.

The results obtained in the present study, both in the validation process and in the verification process, allow for the maximum and minimum temperature scenarios to be possibly used in subsequent studies of extreme events and bioclimatic variables. Future climate scenarios (maximum and minimum temperatures) show an evolution toward warmer climates throughout the Aragón region. These results agree with those obtained from the CMIP5 models by the IPCC (IPCC, 2013) and by the AEMET (www.Aemet.es). Previous data collected by other authors and assembled by the IPCC (IPCC, 2013) expect that the greatest temperature increases will occur during the summer months. The results of the present study showed that increases in temperature (both maximum and minimum) were less marked than those published by the AEMET (for example, our results showed changes of 3.6 and 7 °C at the end of the century, while the AEMET results predicted changes of 4.1 and 8.2 °C under RPC4.5 and RCP8.5 scenarios, respectively), although both our results and the AEMET results suggest that the summer months will be the time during which the most abrupt changes in temperature will be observed, while the winter months will be the time during which the least abrupt changes will be observed.

Results presented by the IPCC came from the ESMs, so they do not have the added value of applying downscaling techniques to obtain results at a local scale. On the other hand, one of the advantages of working with climate-change scenarios is to have the widest range of future projections (using the greatest possible number of climate scenarios and downscaling methodologies). Therefore, the scenarios generated by the AEMET are complementary to those presented here because different statistical downscaling methodologies, as well as different ESMs, have been applied.

Similar processes were carried out in the generation of climate scenarios for Spain published by the AEMET (www.Aemet.es) and in the EsTcena project (Brands et al., 2013; Brands et al., 2011a). Results that were generated by different centres were presented on the basis of different methodologies, including the one used in the present study.

We compared the new scenarios that were based on the models of the fifth report of the IPCC with those published by Ribalaygua (Ribalaygua et al., 2013a), which correspond to the fourth report of the IPCC. We observed that the most recent scenarios trended toward higher temperatures than what was expected in (Ribalaygua et al., 2013a), with greater increases occurring during summer months compared to winter months. For example, for the summer months, the new results expect that for the period 2071–2100, the maximum temperature in the most extreme case will reach up to 7 °C, while those presented by Ribalaygua (Ribalaygua et al., 2013a) for the same period were estimated to reach 5 °C. However, both studies agreed that the northwest and southwest regions would be the most affected by these variations.

In both cases, maximum and minimum temperatures, in view of the validation results and in the face of the same reanalysis of ERA-40, it is justified that the scenarios generated for the fifth IPCC report are more

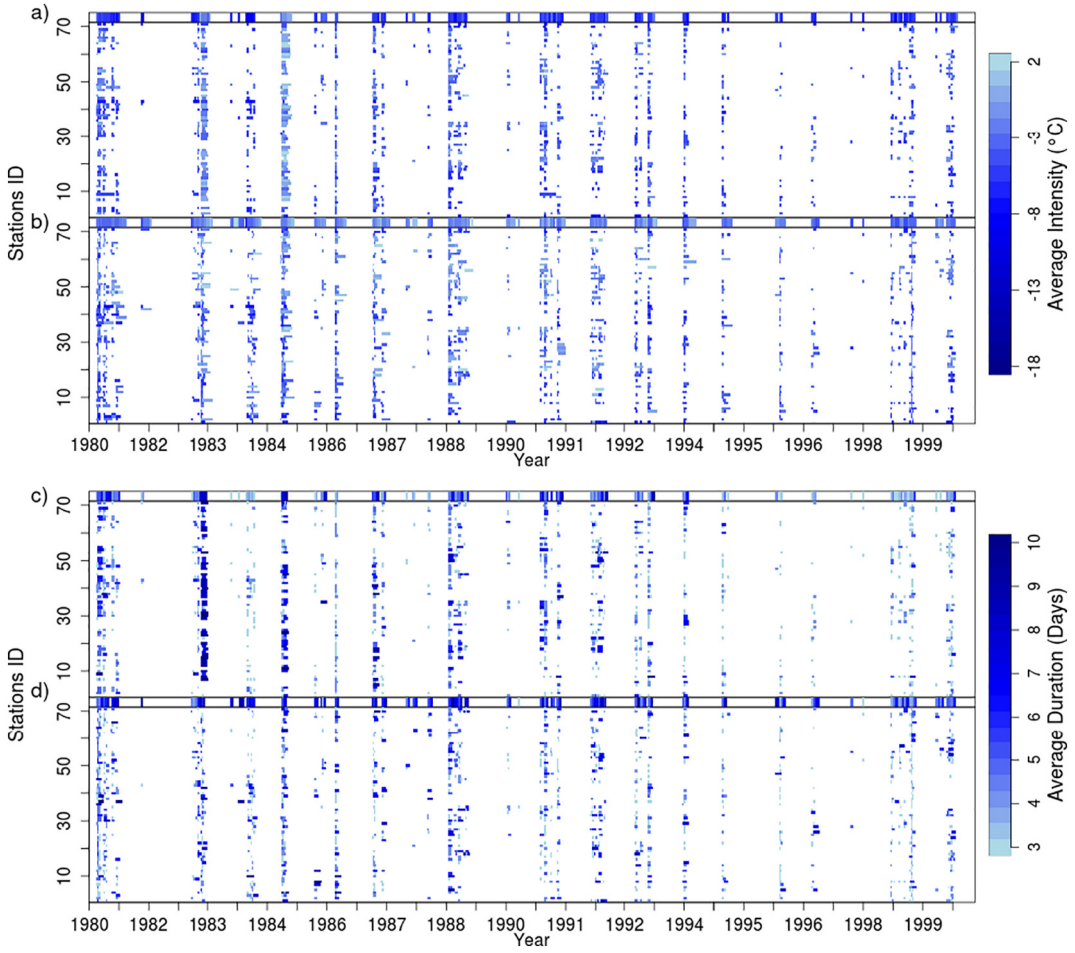


**Fig. 9.** Results of the verification process for cold waves obtained comparing the simulated cold waves for the reanalysis Era40 along the observed cold waves for a common period (1980–2000). a) Average intensity of the heat waves registered in the 71 stations used in the study against b) the average intensity obtained by downscaling of the reanalysis ERA-40 in these stations for the period 1980–2000. The colour of each pixel shows the average intensity that corresponds to each cold wave (°C), each column represents one year of the considered period and each row one station. The upper row shows the mean of the average intensity from the whole observatories. Down, c) and d) same as a) and b) but for the duration of the cold wave. The colour of each pixel shows the duration corresponding to each cold wave (number of days).

precise than those that already exist for the Aragón region. Having a range of climate-scenario projections in Aragón facilitates the evaluation of extreme phenomena of interest, such as heat and cold waves, which have strong impacts in the region.

### *4.2. Consideration about the simulation of heat and cold waves*

Our results allow for the simulation of episodes of heat and cold waves throughout the 21st century and prove the validity of the simulations, as is evident by the good verification and validation results. As the methodology is able to adequately simulate the 95th percentile of maximum temperatures and the 5th percentile of minimum temperatures, it is assumed that the thresholds that define the heat or cold waves are being simulated in an appropriate way.

The downscaling methodology that was used was able to successfully simulate heat and cold waves reported by the observations, as shown by the results of the verification process. The ESMs were also successful at simulating the maximum and minimum temperatures during the validation process. However, in the verification process of heat and cold waves, were identified some limitations that must be considered in the simulation of future scenarios:

1) There were gaps in the observed series. The lack of data in the observed series reduced the length of observed data compared to the reanalysed ERA-40 series (that is, the full series without gaps) for the same period of time. Therefore, the number of days included in the 95th percentile (or 5th percentile) of the maximum (or minimum) temperature was greater in the ERA-40 series compared to the observed series.
2) In general, downscaling techniques tend to soften the simulated temperature series with respect to the observed values, which implies that certain episodes of hot or cold waves are softened in their duration or intensity compared to the observed data and would therefore be classified differently. In the present study, it was appreciated that the average and maximum intensities of the observed cold and heat waves was greater than that simulated for the ERA-40 reanalysis.

In summary, the uncertainties associated with both verification and validation must be considered when interpreting future scenarios.

The results of this study about heat and cold waves are consistent with the results published by both the IPCC (IPCC, 2013) and the AEMET (www.Aemet.es). All models agree that the number of days considered as "hot days" will increase in the coming decades and, therefore, the heat waves will be more frequent. On the other hand, the number of "cold days" will be maintained and, in some cases, will even decrease so, on the contrary of what is expected for heat waves, the frequency of cold waves will remain at its current frequency.

What is stated in the previous paragraph is plausible with one of the main theoretical conclusions about the trend of temperatures reported by the IPCC (IPCC, 2013), which is based on the change in the probability

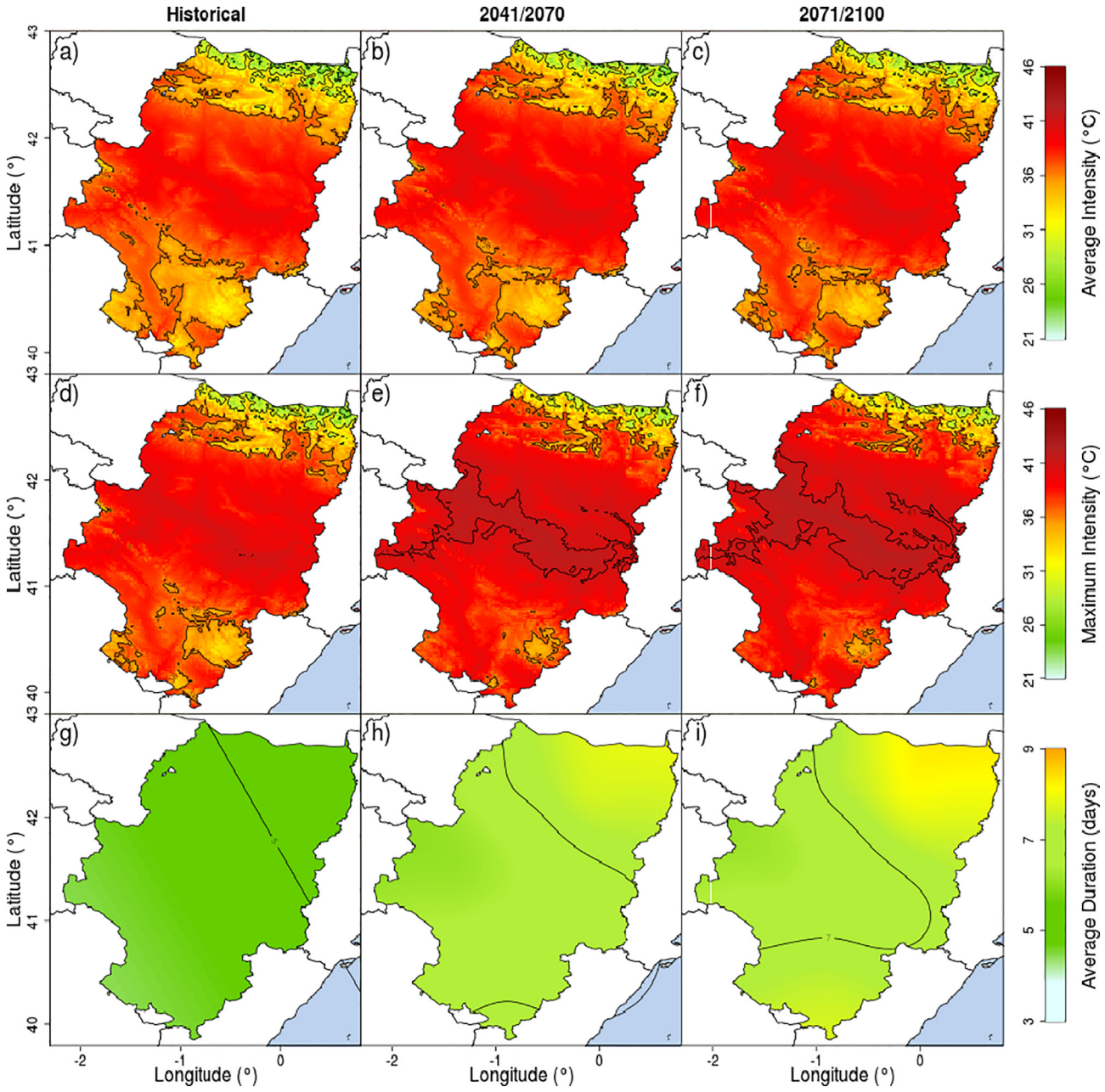


**Fig. 10.** Geographical representation of the expected evolution of the heat waves for Aragon in the periods 2041–2070 and 2071–2100 compared to the reference Historical Period (1971–2000) in terms of absolute values according to the RCP4.5. The rows show the three parameters analysed in the study (average intensity, maximum intensity and duration) and the columns the three temporal periods (Historical, 2041–2070 and 2071–2100). The maps are generated by interpolating the available stations over the entire territory.

of reaching certain temperature values. The probability distribution of temperatures can either move to warmer climates without undergoing changes, can be extended or a combination of both. The third situation is the one that has been observed in recent decades in different studies (Hansen et al., 2012) IPCC, 2001) and is the most plausible situation in the context of the observed data. The new distribution of temperatures implies a less pronounced change in the colder temperatures of the series, a much more marked change in the warmer temperatures and a greater number of warm extreme events. These conclusions support the results anticipated for the coming decades—i.e, the maintenance of cold waves (in number and intensity) and an increase of heat waves.

Regarding the territory of Aragón, the scenarios obtained in the present study indicate that the Ebro valley, the most populated area in the region, will observe the highest maximum temperatures, especially at the end of the century and in the summer (around 40 °C), as well as the greatest intensity of heat waves. This can have important impacts on the health of the population. The health risks associated with heat waves are well known, both in terms of mortality (Robine et al., 2008; Roldan et al., 2016) and mobility (Lin et al., 2009; Steul et al., 2018), as well as health costs (Roldan et al., 2015). Moreover, these extreme events will cause significant socio-economic impacts because a large part of Aragonese industry and farming is situated in this zone (Olesen et al., 2011).

In addition, the Pyrenees will suffer the longest heat waves (but not the most intense ones), especially at the end of the century, and the greatest increases in maximum temperatures with respect to the values recorded during the historical period (1971–2000). The northern zone is where the greatest intensity of cold waves will also be located, although their durations will not change much compared to the current

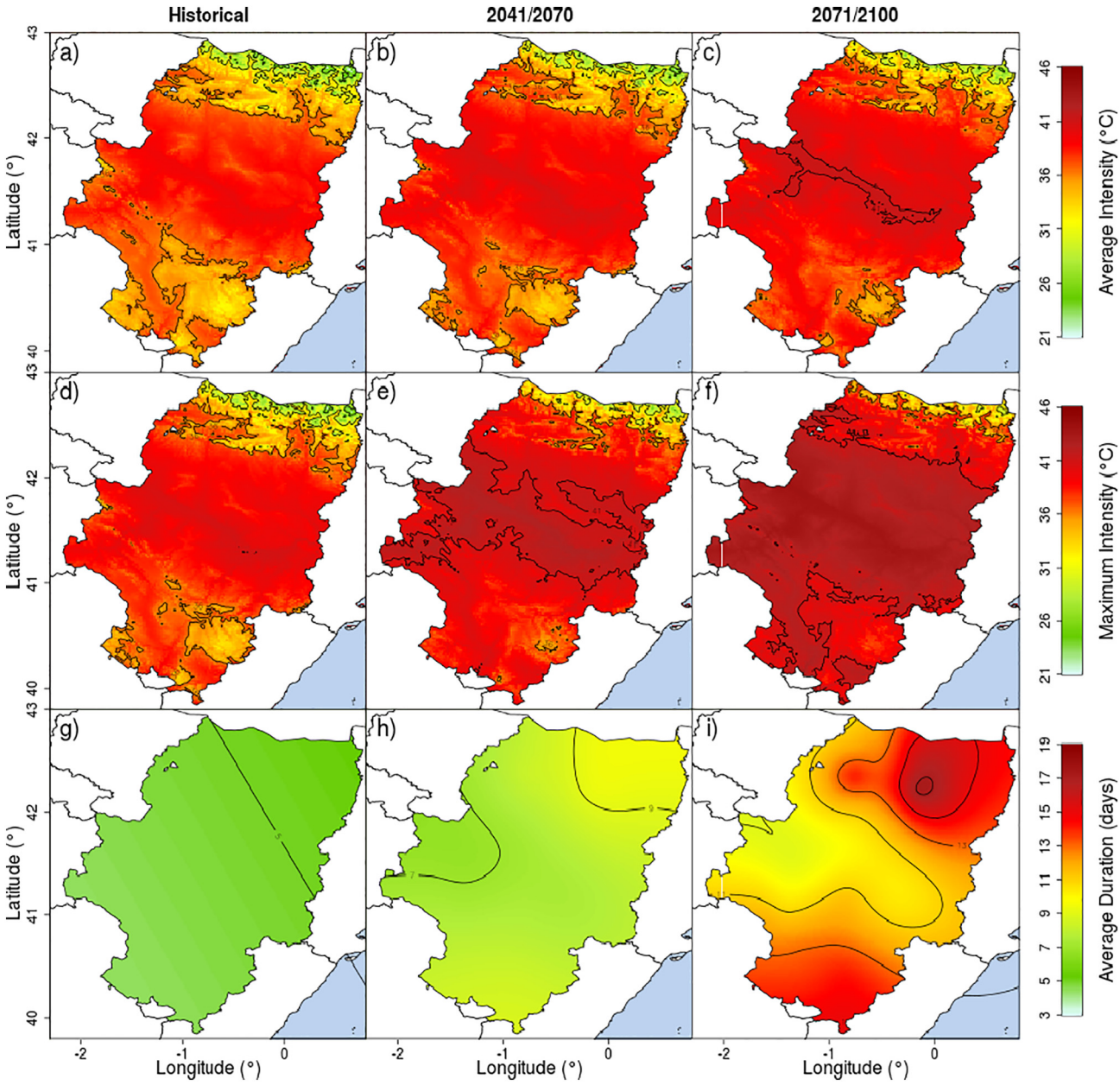


**Fig. 11.** Geographical representation of the expected evolution of the heat waves for Aragon in the periods 2041–2070 and 2071–2100 compared to the reference Historical Period (1971–2000) in terms of absolute values according to the RCP8.5. The rows show the three parameters analysed in the study (average intensity, maximum intensity and duration) and the columns the three temporal periods (Historical, 2041–2070 and 2071–2100). The maps are generated by interpolating the available stations over the entire territory.

cold waves. Therefore, it is the heat that is the most outstanding future risk for these ecosystems.

Changes in temperature (even if they are moderate) and warming are potential risks to this rich ecological area, which is characterised by a diversity of species and a wealth of native plants and animals, giving rise to national parks such as Ordesa and Monte Perdido (high mountains). Therefore, these areas are particularly vulnerable to any changes in climate that could lead to radical alterations in habitats or cause losses in their rich biodiversity, as has been previously described (Kulakowski et al., 2017).

Furthermore, the Pyrenees area decides the amount of water available for urban and agricultural use, with a direct effect on hydrology and agriculture in the Ebro Valley. Changes in temperature and snow accumulation could seriously threaten the sustainability and the equilibrium between available resources and water demand. On the other hand, abrupt temperature changes can lead to accelerated thawing that could cause flooding in populated areas near the river, a risk that has been well evaluated in the literature (Gobiet et al., 2014; Guerreiro et al., 2018) and that will demand new and innovative adaptation strategies (De Martino et al., 2012).

Finally, the disappearance of snow due to a rise in temperature in the area could lead to a negative impact on the winter tourism industry and the Pyrenean ski resorts, which are currently an important part of the region's economy, especially in the Pyrenean valleys (Gilaberte-Burdalo et al., 2014; Gilaberte-Burdalo et al., 2017; Lopez-Moreno et al., 2011; Pons et al., 2015).

## 5. Conclusions

Our study of data from Aragón, Spain, is the first to simulate episodes of heat and cold waves throughout the 21st century in a valid way, based on the good verification and validation results. In addition, we used

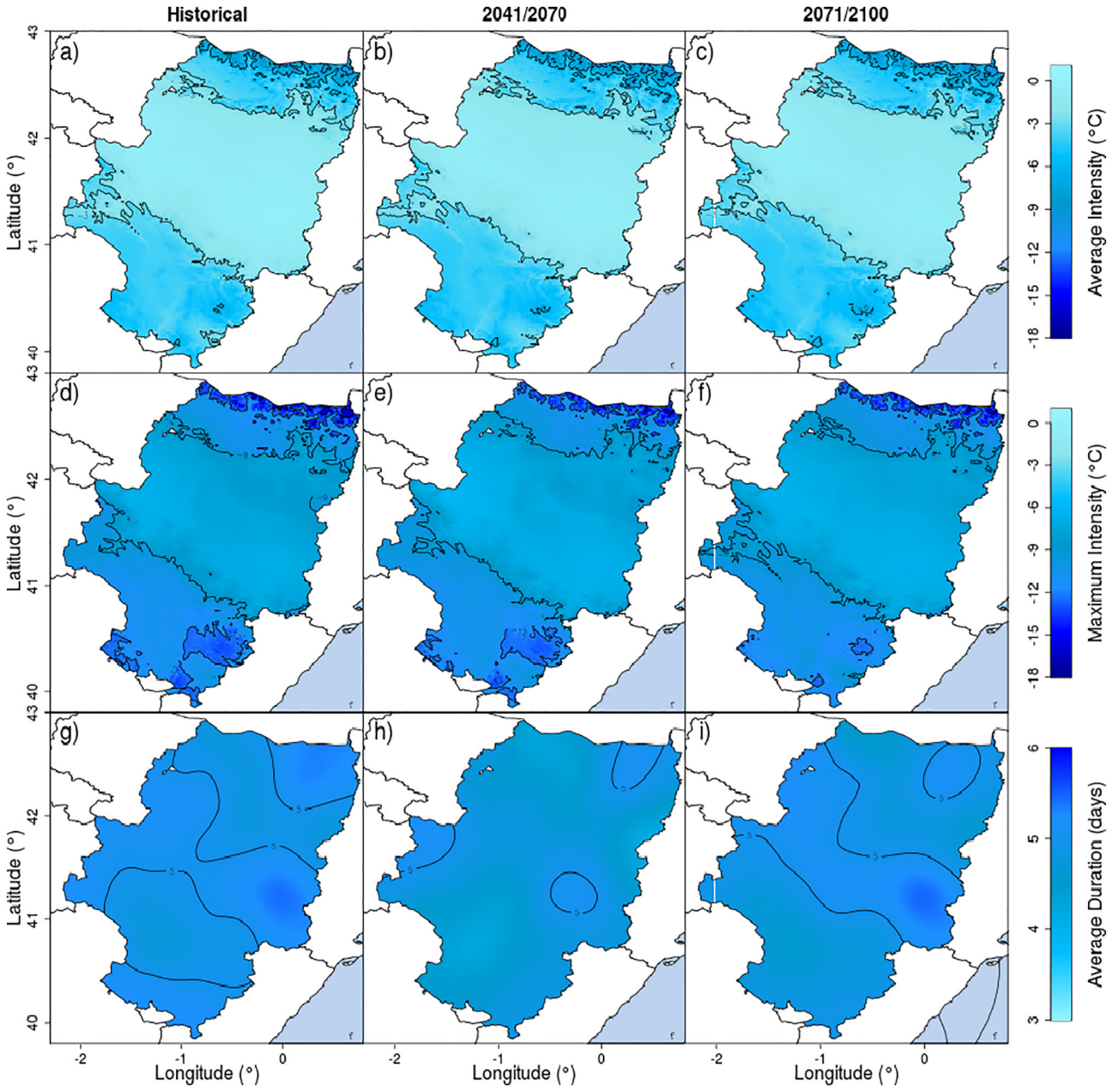


**Fig. 12.** Geographical representation of the expected evolution of the cold waves for Aragon in the periods 2041–2070 and 2071–2100 compared to the reference Historical Period (1971–2000) in terms of absolute values according to the RCP4.5. The rows show the three parameters analysed in the study (average intensity, maximum intensity and duration) and the columns the three temporal periods (Historical, 2041–2070 and 20,712,100). The maps are generated interpolating the available observatories over the entire territory.

climate models to obtain more precise climate scenarios for the temperatures in this territory compared to previously available scenarios.

The use of ESMs from the fifth report of the IPCC and a methodology of downscaling has proven to be effective, allowing us to obtain greater precision in the simulation of the climate variables in this territory and to predict a realistic picture of the risks that extreme temperatures can cause in the Aragón region, both spatially and temporally. The climate scenarios predict higher maximum temperatures compared to previous scenarios. The greatest increases will occur during summer at the end of the century, reaching values of up to 7 °C in the most unfavourable scenario.

Climate heat- and cold-wave scenarios showed that heat waves will be longer and more intense in upcoming decades. However, intensity and duration of cold waves will not change much compared to the current cold waves. The temperatures and heat-wave intensities will be especially high in the Ebro Valley, the most populated area. However, the Pyrenees will suffer the longest heat waves, especially at the end of the century, and the greatest increases in maximum temperatures.

The present study provides useful information coming from the downscaling for the first time in Aragón of models from IPCC5 to support decision-making and in the development of specific measures to prevent socio-economic, environmental and human health impacts due climate change in Aragón, a territory that can be a good indicator of the impacts of climate change in southern Europe.

## Appendix A. Supplementary data

Supplementary data to this article can be found online at https://doi.org/10.1016/j.scitotenv.2018.09.352.

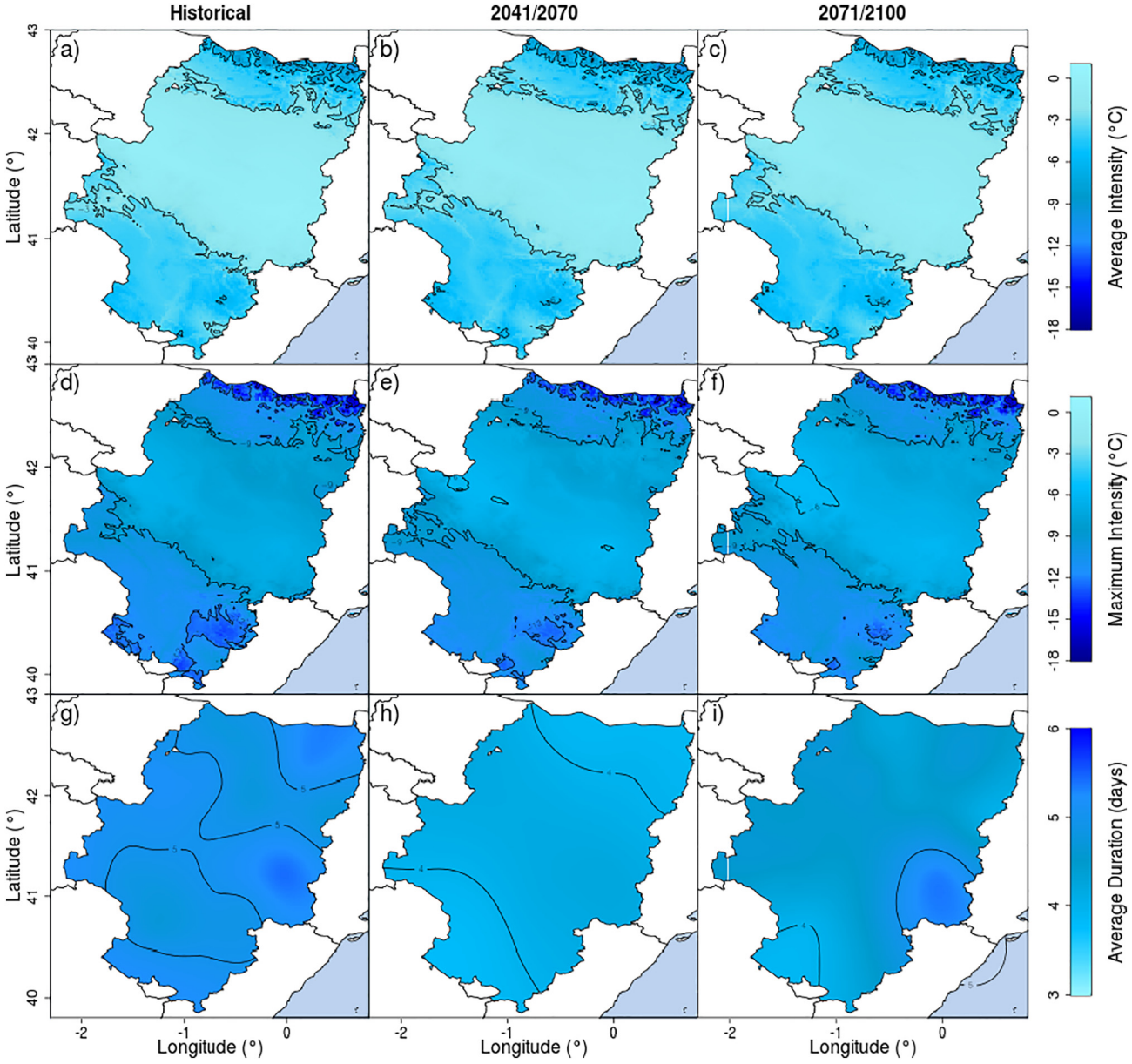


**Fig. 13.** Geographical representation of the expected evolution of the cold waves for Aragon in the periods 2041–2070 and 2071–2100 compared to the reference Historical Period (1971–2000) in terms of absolute values according to the RCP8.5. The rows show the three parameters analysed in the study (average intensity, maximum intensity and duration) and the columns the three temporal periods (Historical, 2041–2070 and 20,712,100). The maps are generated interpolating the available observatories over the entire territory.

## References


Anderson, B.G., Bell, M.L., 2009. Weather-related mortality how heat, cold, and heat waves affect mortality in the United States. Epidemiology 20, 205–213.

Asong, Z.E., Khaliq, M.N., Wheater, H.S., 2016. Projected changes in precipitation and temperature over the Canadian prairie provinces using the generalized linear model statistical downscaling approach. J. Hydrol. 539, 429–446.

Barrera-Escoda, A., Goncalves, M., Guerreiro, D., Cunillera, J., Baldasano, J.M., 2014. Projections of temperature and precipitation extremes in the North Western Mediterranean Basin by dynamical downscaling of climate scenarios at high resolution (1971–2050). Clim. Chang. 122, 567–582.

Benestad, R.E., Hanssen-Bauer, I., Forland, E.J., 2007. An evaluation of statistical models for downscaling precipitation and their ability to capture long-term trends. Int. J. Climatol. 27.

Bentsen, M., Bethke, I., Debernard, J.B., Iversen, T., Kirkevag, A., Seland, O., et al., 2013. The Norwegian Earth System Model, NorESM1-M - part 1: description and basic evaluation of the physical climate. Geosci. Model Dev. 6, 687–720.

Brands, S., Herrera, S., San-Martin, D., Gutierrez, J.M., 2011a. Validation of the ENSEMBLES global climate models over southwestern Europe using probability density functions, from a downscaling perspective. Clim. Res. 48, 145–161.

Brands, S., Taboada, J.J., Cofino, A.S., Sauter, T., Schneider, C., 2011b. Statistical downscaling of daily temperatures in the NW Iberian Peninsula from global climate models: validation and future scenarios. Clim. Res. 48.

Brands, S., Herrera, S., Fernandez, J., Gutierrez, J.M., 2013. How well do CMIP5 Earth System Models simulate present climate conditions in Europe and Africa? Clim. Dyn. 41, 803–817.

Buerger, C.M., Kolditz, O., Fowler, H.J., Blenkinsop, S., 2007. Future climate scenarios and rainfall-runoff modelling in the Upper Gallego catchment (Spain). Environ. Pollut. 148.

Carvalho, D., Rocha, A., Gomez-Gesteira, M., Santos, C.S., 2017. Potential impacts of climate change on European wind energy resource under the CMIP5 future climate projections. Renew. Energy 101, 29–40.

Chen, K., Bi, J., Chen, J., Chen, X., Huang, L., Zhou, L., 2015. Influence of heat wave definitions to the added effect of heat waves on daily mortality in Nanjing, China. Sci. Total Environ. 506-507, 18–25. https://doi.org/10.1016/j.scitotenv.2014.10.092 PMID: 25460935.

Chen, Y.D., Li, J.F., Zhang, Q., 2016. Changes in site-scale temperature extremes over China during 2071–2100 in CMIP5 simulations. J. Geophys. Res.-Atmos. 121, 2732–2749.

Chylek, P., Li, J., Dubey, M.K., Wang, M., Lesins, G., 2011. Observed and model simulated 20th century Arctic temperature variability: Canadian Earth System Model CanESM2. Atmos. Chem. Phys. Discuss. 11, 22893–22907. https://doi.org/10.5194/acpd-11-22893-2011.

Collins, W.J., Bellouin, N., Doutriaux-Boucher, M., Gedney, N., Hinton, T., Jones, C.D., Liddicoat, S., Martin, G., O'Connor, F., Rae, J., Senior, C., Totterdell, I., Woodward, S., Reichler, T., Kim, J., Halloran, P., 2008. Evaluation of the HadGEM2 model. Hadley Centre Technical Note HCTN. vol 74. Met Office Hadley Centre, Exeter, UK.

Cook, J., Nuccitelli, D., Green, S.A., Richardson, M., Winkler, B., Painting, R., Way, R., Jacobs, P., Skuce, A., 2013. Quantifying the consensus on anthropogenic global warming in the scientific literature. Environ. Res. Lett. 8, 024024. https://doi.org/10.1088/1748-9326/8/2/024024.

De Martino, G., De Paola, F., Fontana, N., Marini, G., Ranucci, A., 2012. Experimental assessment of level pool routing in preliminary design of floodplain storage. Sci. Total Environ. 416, 142–147.

Dosio, A., 2017. Projection of temperature and heat waves for Africa with an ensemble of CORDEX regional climate models. Clim. Dyn. 49, 493–519.

Dunne, J.P., John, J.G., Adcroft, A.J., Griffies, S.M., Hallberg, R.W., Shevliakova, E., et al., 2012. GFDL's ESM2 global coupled climate-carbon Earth System Models. Part I: physical formulation and baseline simulation characteristics. J. Clim. 25, 6646–6665.

Estrella, N., Menzel, A., 2013. Recent and future climate extremes arising from changes to the bivariate distribution of temperature and precipitation in Bavaria, Germany. Int. J. Climatol. 33, 1687–1695.

Fernandez-Montes, S., Rodrigo, F.S., 2012. Trends in seasonal indices of daily temperature extremes in the Iberian Peninsula, 1929–2005. Int. J. Climatol. 32, 2320–2332.

Field, C.B., Barros, V., Stocker, T.F., Qin, D., Dokken, D.J., Ebi, K.L., Mastrandrea, M.D., Mach, K.J., Plattner, G.K., Allen, S.K., Tignor, M., Midgley, P.M., IPCC, 2012. Managing the Risks of Extreme Events and Disasters to Advance Climate Change Adaptation. Cambridge University Press, Cambridge, United Kingdom and New York, NY, USA, p. 582.

Fischer, E.M., Schar, C., 2010. Consistent geographical patterns of changes in high-impact European heatwaves. Nat. Geosci. 3, 398–403.

Fonseca, D., Carvalho, M.J., Marta-Almeida, M., Melo-Goncalves, P., Rocha, A., 2016. Recent trends of extreme temperature indices for the Iberian Peninsula. Phys. Chem. Earth 94, 66–76.

Frias, M.D., Fernandez, J., Saenz, J., Rodriguez-Puebla, C., 2005. Operational predictability of monthly average maximum temperature over the Iberian Peninsula using DEMETER simulations and downscaling. Tellus Ser. A Dyn. Meteorol. Oceanogr. 57.

Frias, M.D., Herrera, S., Cofino, A.S., Gutierrez, J.M., 2010. Assessing the skill of precipitation and temperature seasonal forecasts in Spain: windows of opportunity related to ENSO events. J. Clim. 23.

Garcia-Herrera, R., Diaz, J., Trigo, R.M., Hernandez, E., 2005. Extreme summer temperatures in Iberia: health impacts and associated synoptic conditions. Ann. Geophys. 23, 239–251.

Gilaberte-Burdalo, M., Lopez-Martin, F., Pino-Otin, M.R., Lopez-Moreno, J.I., 2014. Impacts of climate change on ski industry. Environ. Sci. Pol. 44, 51–61.

Gilaberte-Burdalo, M., Lopez-Moren, J.I., Moran-Tejeda, E., Jerez, S., Alonso-Gonzalez, E., Lopez-Martin, F., et al., 2017. Assessment of ski condition reliability in the Spanish and Andorran Pyrenees for the second half of the 20th century. Appl. Geogr. 79, 127–142.

Giorgi, F., Gutowski, W.J., 2015. Regional dynamical downscaling and the CORDEX initiative. Annu. Rev. Environ. Resour. 40, 467–490.

Giorgi, F., Mearns, L.O., 1991. Approaches to the simulation of regional climate change - a review. Rev. Geophys. 29, 191–216.

Giorgi, F., Jones, C., Asrar, G.R., 2009. Addressing climate information needs at the regional level: the CORDEX framework. WMO Bull. 58 (3), 175–183.

Gobiet, A., Kotlarski, S., Beniston, M., Heinrich, G., Rajczak, J., Stoffel, M., 2014. 21st century climate change in the European Alps-a review. Sci. Total Environ. 493, 1138–1151.

Goncalves, M., Barrera-Escoda, A., Guerreiro, D., Baldasano, J.M., Cunillera, J., 2014. Seasonal to yearly assessment of temperature and precipitation trends in the North Western Mediterranean Basin by dynamical downscaling of climate scenarios at high resolution (1971–92050). Clim. Chang. 122, 243–256.

Gross, M.H., Alexander, L.V., Macadam, I., Green, D., Evans, J.P., 2017. The representation of health-relevant heatwave characteristics in a regional climate model ensemble for New South Wales and the Australian Capital Territory, Australia. Int. J. Climatol. 37, 1195–1210.

Guerreiro, S.B., Dawson, R.J., Kilsby, C., Lewis, E., Ford, A., 2018. Future heat-waves, droughts and floods in 571 European cities. Environ. Res. Lett. 13.

Hansen, J., Sato, M., Ruedy, R., 2012. Perception of climate change. Proc. Natl. Acad. Sci. U. S. A. 109, E2415–E2423.

Heavens, N., Ward, D., Natalie, M., 2013. Studying and projecting climate change with earth System Models. Nat. Educ. Knowl. 4 (5), 4.

Hertig, E., Seubert, S., Jacobeit, J., 2010. Temperature extremes in the Mediterranean area: trends in the past and assessments for the future. Nat. Hazards Earth Syst. Sci. 10, 2039–2050.

Hervada-Sala, C., Pawlowsky-Glahn, V., Jarauta-Bragulat, E., 2000. A statistical method to downscale temperature forecasts. A case study in Catalonia. Meteorol. Appl. 7.

Imbert, A., Benestad, R.E., 2005. An improvement of analog model strategy for more reliable local climate change scenarios. Theor. Appl. Climatol. 82, 245–255.

IPCC, 2000. Special Report on Emissions Scenarios. Cambridge University Press, Cambridge, UK 0 521 80493 0.

IPCC, 2001. In: Houghton, J.T., Ding, Y., Griggs, D.J., Noguer, M., van der Linden, P.J., Dai, X., Maskell, K., Johnson, C.A. (Eds.), Climate Change 2001: The Scientific Basis. Contribution of Working Group 1 to the Third Assessment Report of the Intergovernmental Panel on Climate Change. Cambridge University Press, Cambridge, UK, and New York, USA.

IPCC, 2013. In: Stocker, T.F., Qin, D., Plattner, G.-K., Tignor, M., Allen, S.K., Boschung, J., Nauels, A., Xia, Y., Bex, V., Midgley, P.M. (Eds.), Climate Change 2013: The Physical Science Basis. Contribution of Working Group I to the Fifth Assessment Report of the Intergovernmental Panelon Climate Change. Cambridge University Press, Cambridge https://doi.org/10.1017/CBO9781107415324.

Iversen, T., Bentsen, M., Bethke, I., Debernard, J.B., Kirkevag, A., Seland, O., et al., 2013. The Norwegian Earth System Model, NorESM1-M - part 2: climate response and scenario projections. Geosci. Model Dev. 6, 389–415.

Jeong, D.I., Sushama, L., Diro, G.T., Khaliq, M.N., Beltrami, H., Caya, D., 2016. Projected changes to high temperature events for Canada based on a regional climate model ensemble. Clim. Dyn. 46, 3163–3180.

Kattenberg, A., Amer Meteorol SOC, 1996. Climate models: projections of future climate. Seventh Symposium on Global Change Studies.

Kent, S.T., McClure, L.A., Zaitchik, B.F., Smith, T.T., Gohlke, J.M., 2014. Heat waves and health outcomes in Alabama (USA): the importance of heat wave definition. Environ. Health Perspect. 122, 151–158.

Kim, S., Sinclair, V.A., Raisanen, J., Ruuhela, R., 2018. Heat waves in Finland: present and projected summertime extreme temperatures and their associated circulation patterns. Int. J. Climatol. 38, 1393–1408.

Knutti, R., Sedlacek, J., 2013. Robustness and uncertainties in the new CMIP5 climate model projections. Nat. Clim. Chang. 3, 369–373.

Kuglitsch, F.G., Toreti, A., Xoplaki, E., Della-Marta, P.M., Zerefos, C.S., Turkes, M., et al., 2010. Heat wave changes in the eastern Mediterranean since 1960. Geophys. Res. Lett. 37.

Kulakowski, D., Seidl, R., Holeksa, J., Kuuluvainen, T., Nagel, T.A., Panayotov, M., et al., 2017. A walk on the wild side: disturbance dynamics and the conservation and management of European mountain forest ecosystems. For. Ecol. Manag. 388, 120–131.

Lavaysse, C., Vrac, M., Drobinski, P., Lengaigne, M., Vischel, T., 2012. Statistical downscaling of the French Mediterranean climate: assessment for present and projection in an anthropogenic scenario. Nat. Hazards Earth Syst. Sci. 12, 651–670.

Lin, S., Luo, M., Walker, R.J., Liu, X., Hwang, S.A., Chinery, R., 2009. Extreme high temperatures and hospital admissions for respiratory and cardiovascular diseases. Epidemiology 20, 738–746.

López, F., Cabrera, M., Cuadrat, J.M., 2007. Atlas Climático de Aragón. First ed. J. Factory, Spain.

Lopez-Moreno, J.I., Goyette, S., Vicente-Serrano, S.M., Beniston, M., 2011. Effects of climate change on the intensity and frequency of heavy snowfall events in the Pyrenees. Clim. Chang. 105, 489–508.

Marsland, S.J., Haak, H., Jungclaus, J.H., Latif, M., Roske, F., 2003. The Max-Planck-Institute global ocean/sea ice model with orthogonal curvilinear coordinates. Ocean Model 5, 91–127.

Miro, J.J., Estrela, M.J., Caselles, V., Olcina-Cantos, J., 2016. Fine-scale estimations of bioclimatic change in the Valencia region, Spain. Atmos. Res. 180, 150–164.

Moss, R.H., Edmonds, J.A., Hibbard, K.A., Manning, M.R., Rose, S.K., van Vuuren, D.P., et al., 2010. The next generation of scenarios for climate change research and assessment. Nature 463, 747–756.

Nychka, D., Furrer, R., Paige, J., Sain, S., 2015. Fields: tools for spatial data. R package version 9.0. (URL: http://doi.org/10.5065/D6W957CT). www.image.ucar.edu/fields.

Olesen, J.E., Trnka, M., Kersebaum, K.C., Skjelvag, A.O., Seguin, B., Peltonen-Sainio, P., et al., 2011. Impacts and adaptation of European crop production systems to climate change. Eur. J. Agron. 34, 96–112.

Parry, M.L., Canziani OF, Palutikof, J.P., Van der Linden, P.J., Hanson, C.E. (Eds.), 2007. IPCC Impacts, Adaptation and Vulnerability Contribution of Working Group II to the Fourth Assessment Report of the IPCC. Cambridge University Press.

Patz, J.A., Campbell-Lendrum, D., Holloway, T., Foley, J.A., 2005. Impact of regional climate change on human health. Nature 438, 310–317.

Perez, J., Menendez, M., Mendez, F.J., Losada, I.J., 2014. Evaluating the performance of CMIP3 and CMIP5 global climate models over the north-east Atlantic region. Clim. Dyn. 43, 2663–2680.

Planton, S., Deque, M., Chauvin, F., Terray, L., 2008. Expected impacts of climate change on extreme climate events. Compt. Rendus Geosci. 340, 564–574.

Pons, M., Lopez-Moreno, J.I., Rosas-Casals, M., Jover, E., 2015. The vulnerability of Pyrenean ski resorts to climate-induced changes in the snowpack. Clim. Chang. 131, 591–605.

R Development Core Team, 2010. R: A Language and Environment for Statistical Computing. R Foundation for Statistical Computing, Vienna, Austria 3-900051-07-0 http://www.R-project.org, Accessed date: 6 July 2011.

Raddatz, T.J., Reick, C.H., Knorr, W., Kattge, J., Roeckner, E., Schnur, R., et al., 2007. Will the tropical land biosphere dominate the climate-carbon cycle feedback during the twenty-first century? Clim. Dyn. 29, 565–574.

Ribalaygua, J., Rosa Pino, M., Portoles, J., Roldan, E., Gaitan, E., Chinarro, D., et al., 2013a. Climate change scenarios for temperature and precipitation in Aragon (Spain). Sci. Total Environ. 463, 1015–1030.

Ribalaygua, J., Torres, L., Portoles, J., Monjo, R., Gaitan, E., Pino, M.R., 2013b. Description and validation of a two-step analogue/regression downscaling method. Theor. Appl. Climatol. 114, 253–269.

Robine, J.M., SLK, Cheung, Le Roy, S., Van Oyen, H., Griffiths, C., Michel, J.P., et al., 2008. Death toll exceeded 70,000 in Europe during the summer of 2003. C. R. Biol. 331, 171-U5.

Roldan, E., Gomez, M., Pino, M.R., Diaz, J., 2015. The impact of extremely high temperatures on mortality and mortality cost. Int. J. Environ. Health Res. 25, 277–287.

Roldan, E., Gomez, M., Pino, M.R., Portoles, J., Linares, C., Diaz, J., 2016. The effect of climate-change-related heat waves on mortality in Spain: uncertainties in health on a local scale. Stoch. Env. Res. Risk A. 30, 831–839.

Russo, S., Sillmann, J., Sterl, A., 2017. Humid heat waves at different warming levels. Sci. Rep. 7.

Saeed, F., Almazroui, M., Islam, N., Khan, M.S., 2017. Intensification of future heat waves in Pakistan: a study using CORDEX regional climate models ensemble. Nat. Hazards 87, 1635–1647.

Schoetter, R., Cattiaux, J., Douville, H., 2015. Changes of western European heat wave characteristics projected by the CMIP5 ensemble. Clim. Dyn. 45, 1601–1616.

Semenov, M.A., Stratonovitch, P., 2010. Use of multi-model ensembles from global climate models for assessment of climate change impacts. Clim. Res. 41, 1–14.

Seubert, S., Fernandez-Montes, S., Philipp, A., Hertig, E., Jacobeit, J., Vogt, G., et al., 2014. Mediterranean climate extremes in synoptic downscaling assessments. Theor. Appl. Climatol. 117, 257–275.

Sillmann, J., Donat, M.G., Fyfe, J.C., Zwiers, F.W., 2014. Observed and simulated temperature extremes during the recent warming hiatus. Environ. Res. Lett. 9.
Smith, T.T., Zaitchik, B.F., Gohlke, J.M., 2013. Heat waves in the United States: definitions, patterns and trends. Clim. Chang. 118, 811–825.
Soares, P.M.M., Cardoso, R.M., Miranda, P.M.A., de Medeiros, J., Belo-Pereira, M., Espirito-Santo, F., 2012. WRF high resolution dynamical downscaling of ERA-interim for Portugal. Clim. Dyn. 39, 2497–2522.
Stegehuis, A.I., Vautard, R., Ciais, P., Teuling, A.J., Miralles, D.G., Wild, M., 2015. An observation-constrained multi-physics WRF ensemble for simulating European mega heat waves. Geosci. Model Dev. 8, 2285–2298.
Steul, K.S., Latasch, L., Jung, H.G., Heudorf, U., 2018. Health impact of the heatwave of 2015: hospital admissions in Frankfurt/Main, Germany. Gesundheitswesen 80, 353–359.
Suparta, W., Yatim, A.N.M., 2017. An analysis of heat wave trends using heat index in East Malaysia. In: Suparta, W., Ismail, M., Abdullah, M. (Eds.), 2017 International Conference on Space Science and Communication. 852.
Taylor, K.E., Stouffer, R.J., Meehl, G.A., 2012. An overview of CMIP5 and the experiment design. Bull. Am. Meteorol. Soc. 93, 485–498.
Tomozeiu, R., Cacciamani, C., Pavan, V., Morgillo, A., Busuioc, A., 2007. Climate change scenarios for surface temperature in Emilia-Romagna (Italy) obtained using statistical downscaling models. Theor. Appl. Climatol. 90, 25–47.
Turco, M., Marcos, R., Quintana-Segui, P., Llasat, M.C., 2014. Testing instrumental and downscaled reanalysis time series for temperature trends in NE of Spain in the last century. Reg. Environ. Chang. 14, 1811–1823.
Uppala, S.M., Kallberg, P.W., Simmons, A.J., Andrae, U., Bechtold, V.D., Fiorino, M., et al., 2005. The ERA-40 re-analysis. Q. J. R. Meteorol. Soc. 131, 2961–3012.
Van der Linden, P., JFB, Mitchell (Eds.), 2009. ENSEMBLES: Climate Change and Its Impacts: Summary of Research and Results From the ENSEMBLES Project. Met Office Hadley Centre, UK , p. 68 160 pp. http://ensembles-eu.metoffice.com/docs/Ensembles_final_report_Nov09.pdf, Accessed date: 10 February 2012.
Vautard, R., Gobiet, A., Jacob, D., Belda, M., Colette, A., Deque, M., et al., 2013. The simulation of European heat waves from an ensemble of regional climate models within the EURO-CORDEX project. Clim. Dyn. 41, 2555–2575.
Voldoire, A., Sanchez-Gomez, E., Melia, D.S.Y., Decharme, B., Cassou, C., Senesi, S., et al., 2013. The CNRM-CM5.1 global climate model: description and basic evaluation. Clim. Dyn. 40, 2091–2121.
Watanabe, S., Hajima, T., Sudo, K., Nagashima, T., Takemura, T., Okajima, H., et al., 2011. MIROC-ESM 2010: model description and basic results of CMIP5-20c3m experiments. Geosci. Model Dev. 4, 845–872.
World Meteorological Organization, 2010. No. 1055. 978-92-63-11055-8 (Switzerland). www.wmo.int.
Xiao-Ge, X., Tong-Wen, W., Jie, Z., 2013. Introduction of CMIP5 experiments carried out with the climate system models of Beijing Climate Center. Adv. Clim. Chang. Res. 4, 41–49. https://doi.org/10.3724/SP.J.1248.2013.041.
Yukimoto, S., Yoshimura, H., Hosaka, M., Sakami, T., Tsujino, H., Hirabara, M., Tanaka, T.Y., Deushi, M., Obata, A., Nakano, H., Adachi, Y., Shindo, E., Yabu, S., Ose, T., Kitoh, A., 2011. Meteorological research institute- earth system model v1 (MRI-ESM1)—model description. Technical Report of MRI. vol 64.
Zittis, G., Hadjinicolaou, P., Fnais, M., Lelieveld, J., 2016. Projected changes in heat wave characteristics in the eastern Mediterranean and the Middle East. Reg. Environ. Chang. 16, 1863–1876.
Zorita, E., von Storch, H., 1999. The analog method as a simple statistical downscaling technique: comparison with more complicated methods. J. Clim. 12, 2474–2489.